Temporal and Spatial Pattern of Sea-level Rise Impacts to Coastal Wetlands and Other Ecosystems.

Haunani H. Kane, Charles H. Fletcher

School of Ocean and Earth Science and Technology, University of Hawaii at Manoa
1680 East-West Road, Honolulu, HI 96822
hkane@hawaii.edu, fletcher@soest.hawaii.edu, (808) 956-3605ph

Pacific Islands Climate Change Cooperative Grant # 6661281

1. ADMINISTRATIVE:

Project title:
Temporal and Spatial Pattern of Sea-level Rise Impacts to Coastal Wetlands and Other Ecosystems.

Recipient:
Charles H. Fletcher
Professor & Associate Dean for Academic Affairs
School of Ocean and Earth Science and Technology, University of Hawaii at Manoa
1680 East-West Road, Honolulu, HI 96822
fletcher@soest.hawaii.edu, (808) 956-2582ph, (808) 956-5512fx

Recipient agency or institution:
University of Hawaii Coastal Geology Group
1680 East-West Rd. POST Room 802, Honolulu, Hawaii, USA

Agreement number:
Pacific Islands Climate Change Cooperative Grant # 6661281

Date of report:
11/15/2013 (draft report)

Period of time covered by the report:
10/1/10-9/31/13

Actual total cost:
$250,000

2. PUBLIC SUMMARY:

Increased water levels, erosion, salinity, and flooding associated with sea-level rise threaten coastal and wetland habitats of endangered waterbirds, sea turtles, monk seals, and migratory shorebirds. As sea-level rises the greatest challenge will be prioritizing management actions in response to impacts. We provide decision makers with two solutions to adaptively manage the impacts of SLR and apply these methods to three coastal wetland environments at Keālia National Wildlife Refuge (south Maui), Kanaha State Wildlife Sanctuary (north Maui), and James Campbell National Wildlife Refuge (north O‘ahu). Firstly, due to the low gradient of most coastal plain environments, the rate of SLR impact will rapidly accelerate once the height of the sea surface exceeds a critical elevation. We calculate a local SLR critical elevation and joint uncertainty that marks the end of the slow phase of flooding and the onset of rapid flooding. This critical transition period provides an important planning target for achieving adaptive management. Secondly, within highly managed coastal areas, landscape vulnerability is related to the site-specific goals of coastal stakeholders. We develop a threat-ranking process that defines vulnerability from a management perspective by identifying those parameters that best characterize how SLR will impact decision maker’s ability to accomplish mandated goals and objectives. We also provide maps of sea-level rise impacts for each wetland that characterize these two

solutions as well as highlight the geographic distribution of potential vulnerabilities. The tools developed here can be used as a guide to initiate and implement adaptation strategies that meet the challenges of SLR in advance of the largest impacts.

3. PROJECT REPORT:

A. TECHNICAL SUMMARY:

The original objectives of this project were to produce map visualizations of sea-level rise (SLR) impacts that have high spatial and temporal specificity such that management decisions with regard to planning for SLR impacts can be made with increased confidence and reliability. In association with these maps, we provide decision makers with additional tools to assess vulnerability of assets due to SLR impacts: 1) definition of a critical threshold of flooding, and 2) the geography of ranked management concerns targeting local conservation goals and objectives. The greatest challenge will be prioritizing long term management actions in response to SLR.

We characterize the site-specific rate of inundation based upon local topography. Due to the low gradient of most coastal plain environments, the rate of SLR impact will rapidly accelerate once the height of the sea surface exceeds a critical elevation. Here we develop this concept by calculating a SLR critical elevation and joint uncertainty that distinguishes between slow and rapid phases of flooding. We apply the methodology to three coastal wetlands environments at Keālia National Wildlife Refuge (south Maui), Kanaha State Wildlife Sanctuary (north Maui), and James Campbell National Wildlife Refuge (north Oʻahu). Using high resolution LiDAR digital elevation models (DEMs), flooded areas are mapped and ranked from high (80%) to low (2.5%) risk based upon the percent probability of flooding under the B1, A2, and A1Fl economic emissions scenarios. Across the critical elevation, the area of wetland (expressed as a percentage of the total) at high risk of flooding under the A1Fl scenario increased from 21.0% to 53.3% (south Maui), 0.3% to 18.2% (north Maui), and 1.7% to 15.9% (north Oʻahu). At the same time, low risk areas increased from 34.1% to 80.2%, 17.7% to 46.9%, and 15.4% to 46.3%, resp. Decision makers have less than 15 years on south Maui, and less than 40 years on North Maui and Oʻahu to conceive, develop, and implement adaptation strategies that meet the challenges of SLR in advance of the largest impacts. Within highly managed areas, landscape vulnerability is related to site-specific goals of decision makers. Building upon prior assessments that define SLR vulnerability based upon elevation alone or as a balance between vertical accretion potential and the changing rate of SLR, we developed a threat-ranking process to aid in the prioritization of coastal wetland conservation actions in response to SLR. Expert knowledge coupled with empirical data is used to identify six input parameters that best characterize how SLR will impact decision maker's ability to accomplish mandated goals and objectives: 1. Type of inundation, 2. Time of inundation, 3. Soil type, 4. Habitat Importance, 5. Infrastructure, 6. Coastal erosion. Through the use of a SLR survey, wetland managers systematically ranked the vulnerability of each input parameter from very high to very low. Type and time of inundation was estimated using robust SLR curves, LiDAR digital elevation models (DEMs), and a hydrologic connectivity method. Poorly drained, high salinity hydric soils, endangered, native, and migrant species habitat, as well as infrastructure flooded by future SLR were also mapped. A geographic information system (GIS) is used to translate the ranking process into a series of maps that identify high vulnerability areas where adaptive management efforts are most needed.

The tools developed in this study can be used as a guide to prioritize conservation actions and initiate decisions to adaptively manage SLR impacts. Conservation strategies will most likely need to be updated to meet the challenges of future SLR impacts. Management will need to determine which areas can be preserved, relocated and some areas may need to be abandoned.

In addition to these two studies, four other studies were published under this funding to improve understanding of SLR impacts. These studies expand the assessment of SLR impacts beyond conservation objectives and investigate other aspects of SLR vulnerability including economic impacts (Cooper et al. 2013a), methodologies of SLR inundation mapping (Cooper et al. 2013b), coastal groundwater impacts (Rotzoll & Fletcher 2012), and the relationship between SLR and historical shoreline change in Hawai'i (Romine et al. 2013). Manuscripts are available at http://www.soest.hawaii.edu/coasts/publications/.

B. PURPOSE AND OBJECTIVES:

The original objectives of this project identified in the proposal were to produce map visualizations of sea-level rise (SLR) impacts that have high spatial and temporal specificity. We targeted key coastal ecosystems on Oahu and Maui that are of high management interest to PICCC members and that have been mapped using LiDAR. We worked closely with stakeholders to define targets, assets of interest, follow-on investigations, develop new modeling approaches and analyze newly revealed characteristics in the inundation scenarios. The outcomes will improve confidence and reliability in making management decisions with regard to planning for the impacts of rising sea level. This is a high priority effort because the rate of global SLR has increased and impacts due to increased inundation are already being seen among Pacific Islands.

Project objectives were met through the development of innovative models. SLR projections used in this study were scaled to meet improvements in regional SLR projections for the Central Pacific. For example regional SLR model projections that take into consideration changes in terrestrial ice mass and thermal expansion of ocean waters predict an end of century sea-level increase 1.0-1.5 m for the Central Pacific (Spada et al. 2013). Thus SLR projections were scaled to target 1.04 m (best case) and 1.43 m (worst case) by 2100 (Vermeer & Rahmstorf 2009).

We characterized the site-specific rate of inundation based upon local topography. Due to the low gradient of most coastal plain environments, the rate of SLR impact will rapidly accelerate once the height of the sea surface exceeds a critical elevation. Here we calculated a SLR critical elevation and joint uncertainty for each study site that distinguishes between slow and rapid phases of flooding. Characterizing flooding into slow and fast phases provides decision-makers with a locally based time frame to implement plans to manage the largest impacts of SLR predicted to occur once the critical elevation is breached.

Within highly managed areas, landscape vulnerability is related to site-specific goals of decision makers. We present a vulnerability-ranking process to aid in the prioritization of coastal wetland conservation actions in response to SLR. Expert knowledge is elicited and vulnerability is defined from a management perspective by identifying those parameters that best characterize how SLR will impact

decision maker's ability to accomplish mandated goals and objectives. Vulnerability parameters for each study site are used in a GIS to combine parameters and produce a final vulnerability map.

C. ORGANIZATION AND APPROACH:

1. Identifying appropriate SLR projections

1.1 Spatial variability of SLR

SLR projections and current rates are often described in a global context, however in reality there are spatial variations of SLR superimposed on a global average rise (Sallenger et al. 2012). Local or relative sea-level depends upon a number of different factors including changes in terrestrial ice mass (e.g. melting of glaciers and ice sheets), changes ocean temperature, and glacial isostatic adjustment (GIA).

As glaciers and ice sheets melt, they directly add fresh water to the ocean increasing sea-level. Due to gravitational forces, land ice attracts ocean water and when it melts the gravitational attraction of the ice sheet weakens decreasing the relative sea-level near the ice in the polar regions and increasing sea-level in the far field near the tropics (Spada et al. 2013). Recent studies show that all alpine glacial regions as well as the Antarctic and Greenland ice sheets are losing mass (Figure 1; Figure 2) (Gardner et al. 2013; Rignot et al. 2011).

Increases in atmospheric temperature warm seawater, increasing its volume and subsequent sea-level, a process known as thermal expansion. Climate models predict that even if greenhouse gas emissions cease rising and some excess CO_2 is removed from the atmosphere, SLR will persist for many centuries due to thermal expansion of deep ocean water (Meehl et al. 2012).

GIA is the response of the Earth's crust to changes in ice mass throughout the last glacial cycle. Approximately 20,000 years ago during the last glacial maximum large portions of the northern hemisphere were covered by continental glaciers, which caused a redistribution of Earth's internal mass and surface (Slangen et al. 2012). As the ice began to melt there was a delayed (viscoelastic) response of the lithosphere that continues to this day.

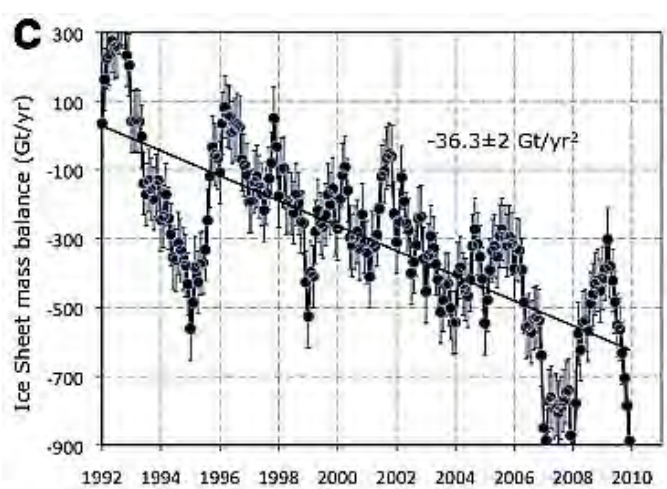

Figure 1. Total ice sheet mass blance (dm/dt) between 1992 and 2009 for Greenland and Antarctica (Rignot et al. 2011). The acceleration in ice sheet mass balance measured in gigatons per year squared is noted in the figure.

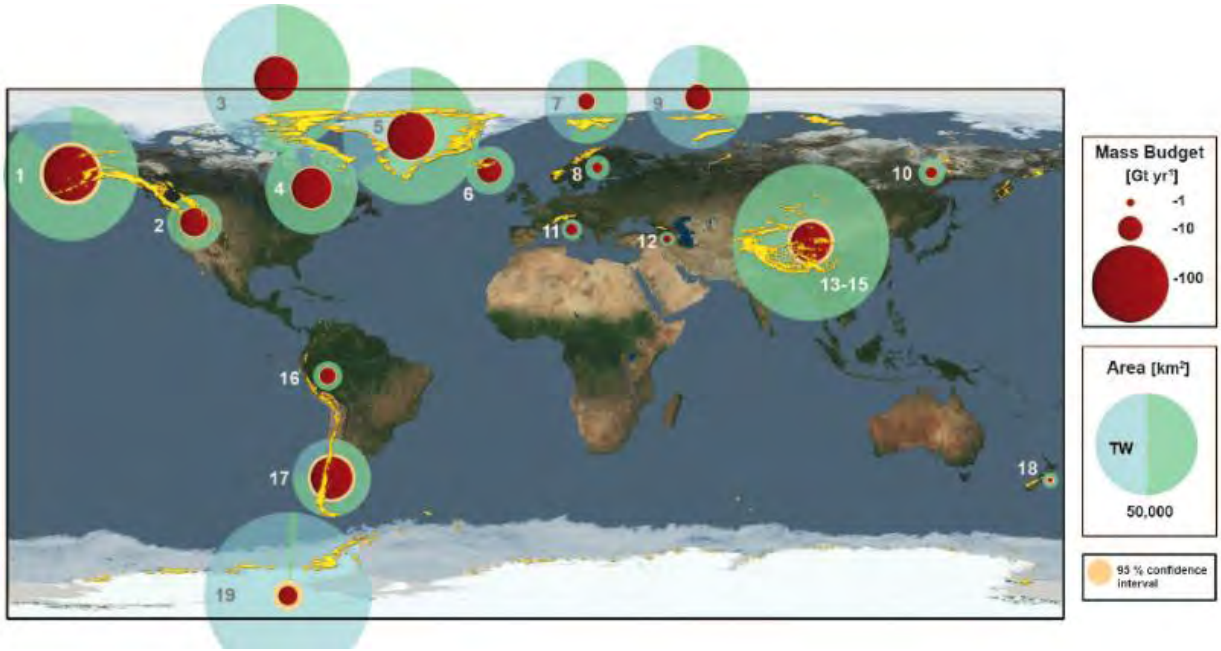

Figure 2. Regional glacier mass budgets and areas (Gardner et al. 2013). Red circles show 2003-2009 regional glacier mass budgets, and light blue/green circles show regional glacier areas with tidewater basin fractions (the extent of ice flowing into the ocean) in blue shading. The 95% CI in mass change estimates is represented by peach but is visible only in regions with large uncertainties.

In addition to changes in ice mass, ocean responses, and GIA, local subsidence also plays a role in sea-level variability among the Hawaiian Islands. Lithospheric plate flexure related to volcanism at the Hawaiian hotspot, causes subsidence of younger shield volcanoes. This is due to rapid loading of the lithosphere by growing volcanoes (Moore, 1987.) SLR rates recorded at tide gauges are similar for the older islands of Kaua‘i and O‘ahu (Kaua‘i: 1.53 ± 0.59 mm/yr and 1.50 ± 0.25 mm/yr, resp.) and higher at Maui and Hawai‘i Island (Maui: 2.32 ± 0.53 mm/yr, 3.27 ± 0.7 mm/yr, resp.) (http://tidesandcurrents.noaa.gov; Romine et al. 2013) (Figure 3). While tide gauge records provide a continuous history of sea-level at a specific location, satellite altimeter missions measure sea surface heights with near global coverage every 10 days from 1993 to present. SLR observed for Maui and Hawai‘i is greater than the linear global trend of 1.7 ± 0.2 mm/yr from 1900 to 2009 based upon tide gauges (Church and White 2011). Only Hawai‘i island is currently experiencing a rate of SLR comparable to the short-term global trend of 3.2± 0.4 mm/yr recorded by satellite data (Church and White 2011). While hotspots of accelerated sea-level rise have been recorded in other areas (e.g. Atlantic coast of North America) (Sallenger et al. 2012), acceleration has not yet been detected in Hawai‘i tide gauge records, and is likely related to climatological variability (e.g. tradewinds; Merrifield and Maltrud 2011).

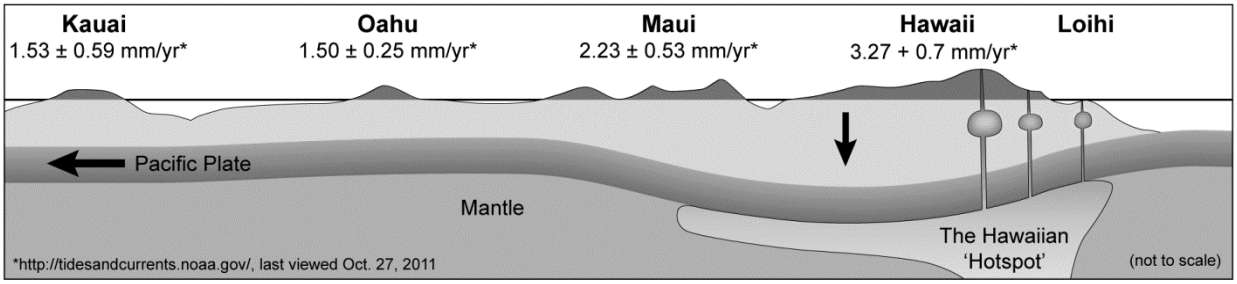

Figure 3. Mean sea-level trends recorded at local tide stations (modified after Romine *et al* 2013).

1.2 Current SLR models

The spatial variability of end of the century sea-level has been modeled by two regional SLR models. A coupled global circulation model predicts that under scenarios of rapid melting Central Pacific sea-level by the end of the century will be 1.12-1.17 m above present (Slangen et al. 2012) (Figure 4). A second regional model by Spada et al. *(*2013), improves upon terrestrial ice mass estimates and concludes that terrestrial ice mass is the main source of SLR rather than the ocean response as modeled by Slangen et al. (2012). Considering both terrestrial ice mass and ocean response contributions to SLR, a mid range model predicts an end of century sea-level increase of 0.5-0.75 m and the high end model predicts an increase of 1.0-1.5 m for the Central Pacific (Spada et al. 2013) (Figure 5). The value of regional sea-level rise models is that they allow us to infer the Hawaiian Islands departure from the global average. Yet it has been argued that regional SLR models are not yet ready for direct use because they fail to capture observed local weather patterns, local subsidence, produce inconsistencies among projections, and are not associated with a SLR curve from which we can produce yearly SLR values (Tebaldi et al. 2012).

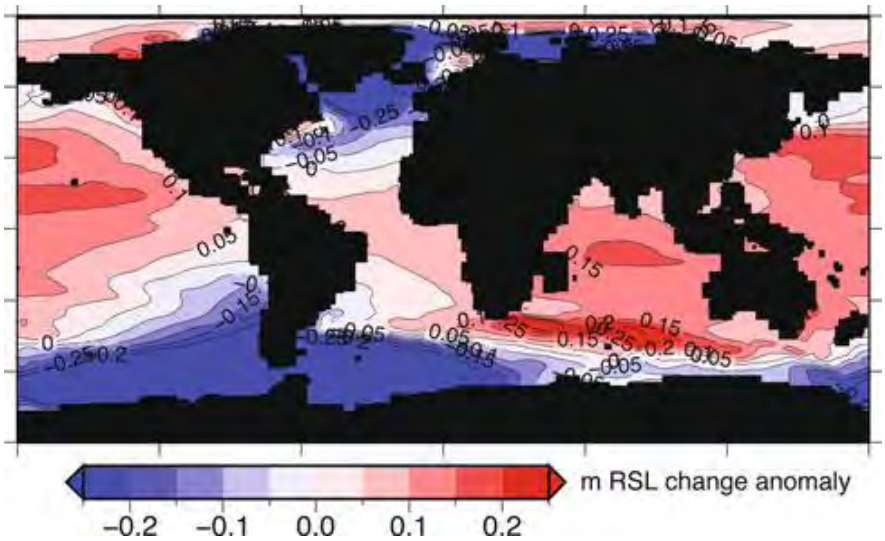

Figure 4. Mean seasonal sea-level anomaly (m) with respect to a global mean regional sea-level change of 1.02 m for the year 2100 (Slangen et al. 2011). Sea-level in Hawai'i is predicted to be 0.1-0.15 m above the global average, corresponding to a 1.12-1.17 rise in total sea-level.

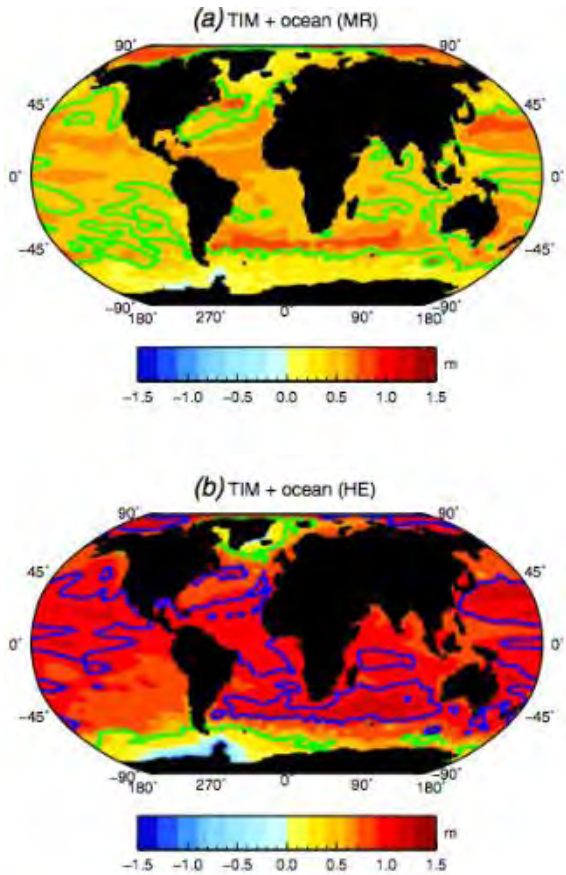

Figure 5. Total sea-level rise for the year 2100 based upon the (a) MR (mid-range) and (b) HE (high-end) sea-level rise scenarios (Spada et al. 2012). The green contour line corresponds to a 0.5 m rise in sea-level and the blue line corresponds to a 1.0 m rise in sea-level. Hawai'i is predicted to experience a 0.5-0.75 rise in total sea-level under the ME scenario, and a 1.0-1.5 rise in sea-level under the HE scenario.

A number of global SLR estimates have been created for the year 2100 and beyond using physical modeling (e.g.: Slangen et al. 2012, Spada et al. 2013), semi-empirical methods (eg: Vermeer and Rahmstorf 2009; Jerejeva et al. 2012), and expert judgment assessment (Bamber and Aspinall 2013) (Table 1). Semi-empirical and expert judgment methods serve as alternatives to models based on physical processes because dynamic systems such as ice sheets are not yet fully understood (IPCC, 2007; Vermeer et al,. 2012). In particular the semi-empircal method of Vermeer and Rahmstorf (2009) offers a unique solution for the position of future sea-levels by providing yearly global values for multiple economic emission scenarios. Vermeer and Rahmstorf (2009) compute mean sea-level curves and associated uncertainty (1σ) bands across the 19 climate models used in the Intergovernmental Panel on Climate Change (IPCC) fourth assessment report (AR4) (2007) (Figure 6). The robustness of Vermeer and Rahmstorf's (2009) projections of future SLR are documented by Rahmstorf et al, (2011).

Table 1. Sea-level (m) estimates for the year 2100 based upon expert judgment assessment, semi-empirical methods, and physical modeling methods.

Expert judgment assessment		Semi-empirical		Physical (Ocean coupled model)		
Bamber and Aspinall (2013)	National Research Council (NRC) (2012)	Vermeer & Ramstorf (2009)	Jerejeva (2010)	*Slangen et al. (2012)	*Spada et al. (2013)	IPCC AR5 (2013)
0.33 – 1.32 m	0.5 - 1.4 m	0.75 - 1.9	0.6-1.9 m	1.12 – 1.17	0.5 –1.5	0.26 -0.98

*Central Pacific sea-level estimate. All other sea-level rise projections are global estimates.

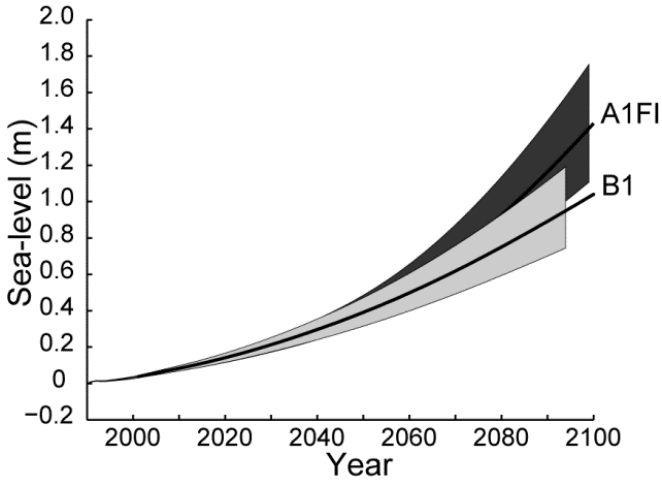

Figure 6**.** SLR projection 1990-2100 for the B1 (1.04 m by 2100), and A1FI (1.43 m) economic scenarios (modified after Vermeer and Rhamstorf 2009).

The IPCC's fifth assessment report (AR5) released in September 2013 builds upon AR4 and incorporates new evidence of climate change, including SLR data (IPCC 2013). Improved understanding of the physical components of SLR, better agreement among process-based models with observations, and improved modeling of land-ice contributions has resulted in more robust SLR predictions. A new set of scenarios, the Representative Concentration Pathways (RCPs) was used to model climate for the end of the 21st century (2081-2100) relative to 1986-2006. AR5 predicts that global mean SLR for 2081-2100 will likely be in the range of 0.26-0.55 m for the best case scenario (RCP2.6) and 0.45 to 0.82 m for the worst case scenario (RCP 8.5). By the end of the century RCP 8.5 projects a 0.98 rise in global mean sea-level.

Due to the lack of a regional SLR model for Hawai'i and the recent release of the AR5 projections in comparison to the timeline of this project we apply Vermeer and Rahmstorf's B1 and A1FI SLR scenarios. The B1 (1.04 m), or best case scenario embodies a more environmentally stable future characterized by reductions in material intensity, introduction of more efficient technologies, and a mid-

century peak in population that rapidly declines. For a future of rapid warming and melting, global SLR projections are converging upon an estimate of 1 m by 2100 (eg. Fletcher 2009; Rahmstorf 2010; Nicholls 2011; NRC 2012; Cooper et. al 2013b) (Table 1). The A1FI (1.43 m by 2100) or worst case scenario represents a fossil fuel intensive future characterized by rapid economic growth, and a population growth equivalent to B1. The A1FI scenario also estimates the upper range of sea-level projected for the Central Pacific by regional SLR models. The methodology applied in this study is flexible and structured such that it may be updated as new SLR projections are made available.

2. Previous studies that assess wetland vulnerability to SLR impacts

A recent study suggests that 20% of the world's wetlands may be lost to SLR by the year 2080 (Nicholls 2004). Wetland vulnerability is often determined by whether sediment accretion on the surface of a wetland can keep pace with the rate of sea-level rise (Webb et al. 2013). Wetlands accrete vertically in two ways: 1. entrapping sediment deposited by tidal waters and storms, and 2.preservating below ground biomass in the form of peat. Micro-tidal (<2 m) marshes like those in Hawaiʻi are believed to be more susceptible than Macro (>4 m) and meso-tidal (2-4 m) marshes because they receive lower sediment loads from the ocean and are more dependent upon organic matter accumulation to support vertical accretion (Stevenson and Kearney 2009). Vertical accretion rates in the shallow subsurface and surface may be measured using a Surface Elevation Table (SET) and marker horizons (e.g. Morris et al. 2002; Webb et al. 2013). The SET is a benchmark rod that is driven through the soil profile (approximately 10-25 m) and equipped with a horizontal arm to measure the distance to the substrate surface from a specified elevation. The SET is usually accompanied by artificial marker horizons made of feldspar or sand to monitor surface elevation change.

In addition to increased water levels, wetlands are also vulnerable to increased salinity via marine overwash or subsurface saltwater intrusion. At most coastal wetlands the dune system acts as a natural barrier to marine flooding, however as sea-level rises and coastal erosion increases, the dunes may be breached allowing salty surface waters to penetrate inland wetlands. Many of the managed wetlands in Hawaiʻi require groundwater to supplement pond water levels during the dry season (USFWS 2011a, 2011b). However, pumping of freshwater to wetlands creates a cone of depression allowing for increased saltwater intrusion to the wetlands, which may be exacerbated by SLR. This practice should be further studied by groundwater hydrologists with the goal of quantifying the depth of the freshwater lens and timing of future salinization.

Coastal wetland loss due to sea-level rise can be offset to some extent by inland wetland migration as tidal marsh plants replace upland species (Osgood and Sillman 2009). Wetland vulnerability can be addressed by numerical modeling of ecological feedbacks as sea-level increases (e.g. Kirwan & Temmerman 2009; Kirwan et al. 2010). In particular, the Sea Level Affecting Marshes Model (SLAMM 6) simulates changes in tidal marsh area and habitat type in response to sea-level rise by accounting for inundation (rise in water levels and salt boundary), erosion, overwash (beach migration and transport of sediment), saturation (upland migration of swamps and marshes), and vertical accretion of wetlands.

The SLAMM model was applied through an independent study (e.g. Clough & Larson 2010a,b) to five Hawaiian U.S. Fish and Wildlife Service (USFWS) National Wildlife Refuge (NWR) wetlands using

the A1B IPCCC Fourth Assessment Report (2007) economic emission SLR scenario. The model simulated SLR at 0.39, 0.69, 1.0, 1.5, and 2.0 m, and habitat change was mapped at 25 year increments up to 2100. Vertical accretion values were not available for any of the Hawaiian wetlands so default values were assumed. The fraction of wetland that is lost (or transferred to the next habitat class) is calculated as a function of the slope of the cell, the minimum elevation for that wetland, and the lower elevation boundary for that wetland (Clough et al. 2010c). Results for Keālia Pond NWR (S. Maui), and James Campbell NWR (N. O'ahu) are shown in Table 2 (Clough & Larson 2010a,b) as these two study areas were included in our SLR assessment. Habitat switching may be specified as a function of salinity, however this option was not employed for Hawaiian wetlands.

Table 2. Predicted loss of land categories derived from SLAMM

	SLR (m)									
	James Campbell					Keālia				
Land Categories	**0.4**	**0.7**	**1**	**1.5**	**2**	**0.4**	**0.7**	**1**	**1.5**	**2**
Undeveloped Dry Land	4%	14%	24%	39%	54%	0%	3%	27%	70%	91%
Inland Fresh Marsh	5%	21%	33%	48%	62%	1%	6%	16%	61%	83%
Developed Dry Land	1%	6%	13%	23%	32%	0%	0%	0%	49%	91%
Swamp	-	-	-	-	-	0%	4%	6%	40%	84%

This study builds upon the work done by SLAMM in a number of ways including but not limited to:

1. In addition to modeling SLR impacts at James Campbell and Keālia we have expanded the study area to also include Kanaha Pond State Wildlife Sanctuary, which was not included in the SLAMM 6 study.
2. We modeled SLR impacts at a higher spatial resolution (2 m horizontal resolution DEMs for all three study areas versus a 5 m DEM at James Campbell and a 15 m DEM at Keālia).
3. Diked areas were not included in SLAMM's analysis, however we employ hydroflattening in our vulnerability map to model SLR impacts at at diked areas.
4. With the assistance of modern aerial images and figures provided by wetland managers at Keālia and Kanaha we improved the boundaries of wetlands as defined by the 1976 National Wetland Inventory (NWI) wetland layers. The SLAMM 6 study acknowledged that the NWI layers introduced a considerable amount of uncertainty regarding wetland type and location.
5. The critical elevation assessment adds another temporal component to the SLAMM study by identifying a time period in which the rate of flooding is expected to transition from a slow phase of flooding to a rapid phase of flooding.
6. The threat-ranking process employed in the second half of this study allows vulnerability to be defined from a management perspective by identifying those parameters that best characterize how SLR will impact a decision maker's ability to accomplish mandated goals and objectives. This process incorporates and maps the expert knowledge of local wetland managers which is often overlooked in other methodologies.

3. Data analysis

3.1. Identifying study sites

In conjunction with the Hawai‘i Wetland Joint Venture, a group that represents state, federal, and local wetland interests, three coastal wetland environments were identified for this study: James Campbell National Wildlife Refuge (north O‘ahu), Kanaha Pond State Wildlife Sanctuary (north Maui), and Keālia Pond National Wildlife Refuge (south Maui) (Figure 7). Study sites were selected based upon the biological integrity of managed resources within an area, the existence of experienced and knowledgeable management staff, and the availability of mapable layers such as high resolution LiDAR data. All three wetlands are intensively managed throughout the year to restore and maintain self-sustaining populations of endangered waterbirds.

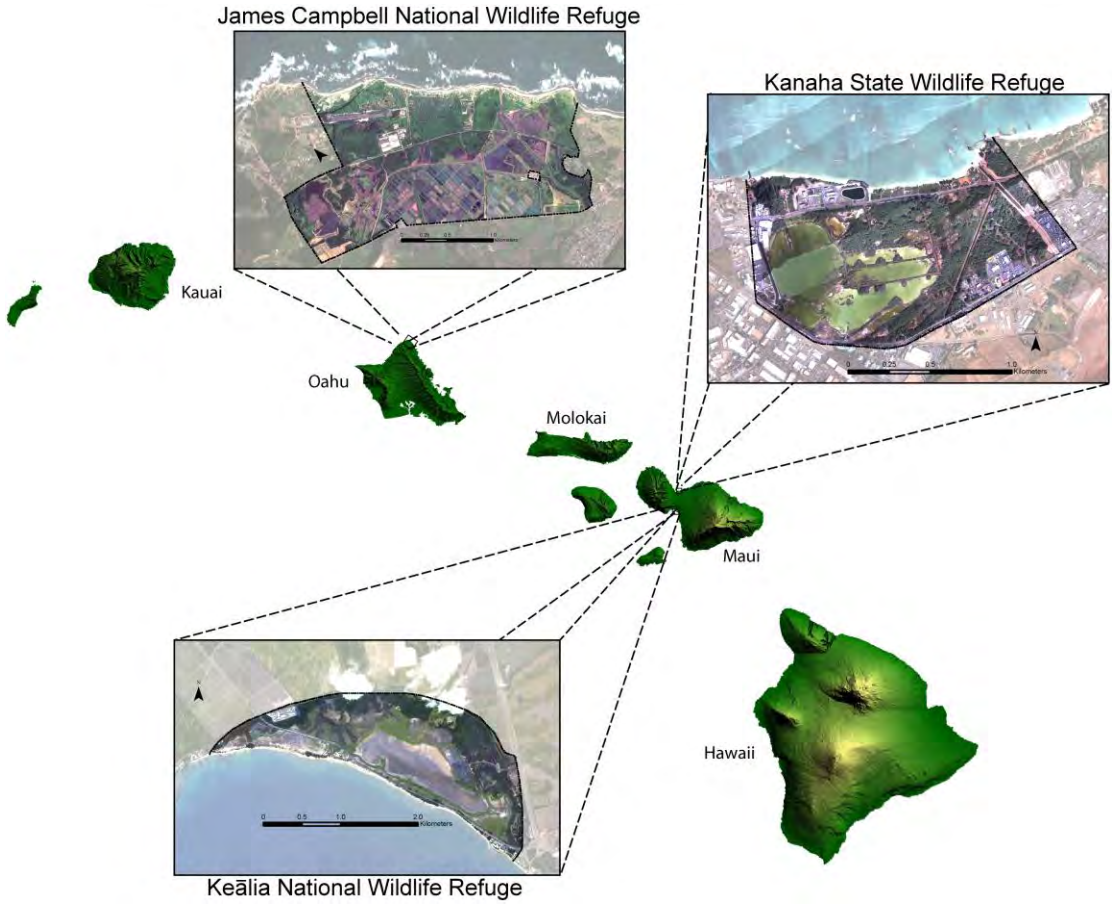

Figure 7. Sea-level rise impacts were assessed for James Campbell National Wildlife Refuge (north O‘ahu), Kanaha Pond State Wildlife Sanctuary (north Maui), and Keālia Pond National Wildlife Refuge (south Maui). In some cases the study area extent included in this assement may encompass more than the Refuge/Sanctuary areas.

Groundwater springs, rainfall, and runoff feed these wetlands, however during the dry season managers may supplement pond water levels with additional sources of groundwater. Unlike temperate salt marshes, Hawai‘i’s coastal wetlands are microtidal, largely isolated from the ocean, and sediment sources include eolian dust, intermittent stream flooding during the wet season (October-April), and internally produced organic solids (U.S. Fish and Wildlife Service 2011a).

With the exception of narrow ocean outlet ditches, the study sites are buffered from marine impacts by 2-4 m sand dunes and a narrow coastal strand. Depending upon the coastal strand for critical habitat are native plants, the endangered Hawaiian monk seal (*Monachus schauinslandi*), the threatened Hawaiian green sea turtle (*Chelonia mydas*), and migrant shorebirds during winter months.

3.2. Mapping the risk of flooding

The U.S. Army Corps of Engineers (USACE) collected airborne LiDAR data for James Campbell and Kanaha during January and February 2007. USACE metadata reports an average point spacing of 1.3 m and a vertical accuracy of better than $\pm$ 0.20 m (1σ). Airborne 1 collected LiDAR for Keālia in 2006 for the Federal Emergency Management Agency (FEMA) and reports average point spacing close to 0.30 m and an $RMSE_z$ of 0.18 m (Dewberry 2008). For the purpose of this study we assume the $RMSE_z$ and 1σ are equivalent (NOAA 2010). LiDAR data was collected in geographic coordinates and ellipsoid heights relative to the North American Datum of 1983 (NAD83) and converted to orthometric heights using the Geiod03 model. These heights were adjusted to mean sea-level based upon a 2006 epoch for the USACE dataset and a 2002 epoch for the FEMA dataset. Last return features, or bare earth LiDAR were converted from LAS format to ESRI shapefile format and reprojected to Universal Transverse Mercator (UTM) zone 4 North.

Triangular irregular networks (TIN) were derived from the processed and filtered LiDAR point data for each study area. To identify areas where point density poorly characterizes coastal morphology, a distance of 20 m (maximum edge length) was used to constrain the TIN extents. A 2 m horizontal resolution DEM was interpolated from each TIN using the nearest neighbor method to represent the corresponding bare earth topography.

We account for the uncertainty of SLR projections and LiDAR data in our SLR flood maps using a combination of several existing standards. Areas of high (80-100% probability), moderate (50-100% probability), and low (2.5-100% probability) risk are mapped using cumulative percent probability. The 80% probability contour identifies high confidence flood areas (NOAA 2010), while the 50% rank maps the area flooded by the predicted sea-level value alone. Gesch (2009) and the National Standard for Spatial Data Accuracy (FGDC 1998) recommend the use of the linear error at the 95% confidence level (1.96 x $RMSE_z$) to identify additional areas that may be inundated at time *t*. The 2.5% rank used in this study to identify low risk areas equates to a standard-score of 1.96 when a cumulative or single tail approach is used (NOAA 2010).

To assess the percent probability that a location (x,y) is inundated at time *t* we adhere closely to NOAA (2010) and Mitsova et al. (2012). For each economic scenario a 2 m horizontal resolution raster is created to calculate the expected height above MHHW (μ_h) at time *t*. We take the difference between the projected sea-level value above MHHW (μ_s) and the DEM elevation (μ_z):

$$\mu_h = \mu_s - \mu_z \tag{1}$$

To account for the uncertainty (σ_t) associated with an area's expected height above MHHW we combine two random and uncorrelated sources using summing in quadrature (Fletcher et al. 2003): SLR model uncertainty (σ_s) and LiDAR vertical uncertainty (σ_z).

$$\sigma_t = \sqrt{{\sigma_s}^2 + {\sigma_z}^2} \quad (2)$$

The SLR model uncertainty reflects a semi-empirical characterization of the physical link between climate change and SLR, and the LiDAR uncertainty is a measure of the vertical accuracy of the LiDAR points to represent the corresponding bare earth topography. A second surface is created to represent the standard-score (SS_{XY}) or the number of standard deviations a value falls from the mean.

$$SS_{XY} = \frac{\mu_h}{\sigma_t} \quad (3)$$

The standard-score raster is reclassified to a percent probability raster by means of a look-up table assuming normally distributed errors. Under each phase of SLR, we map and calculate the percent area with low, moderate, and high risk of flooding for the B1 (1.04 m by 2100), and A1FI (1.43 m) scenarios. Re-engineered areas such as the diked ponds at James Campbell are not included in the critical elevation analysis but are considered in the second portion of this study (using ranked management concerns to define vulnerability).

4. Identifying a local SLR critical elevation

We use a land area hypsometric curve (Zhang 2011; Zhang et al. 2011) to identify a critical elevation and characterize the rate of flooding based upon local topography (Figure 9). We adhere closely to NOAA Coastal Services Center Coastal Inundation Toolkit Mapping Methodology (accessed at http://www.csc.noaa.gov/slr/viewer/assets/pdfs/Inundation_ Methods. pdf) and model the area flooded at 0-5.0 m using the DEMs. It is important to note that in some areas the extent of the study area analyzed may encompass more than the managed refuge or sanctuary areas. Figure 7 depicts the study area boundaries.

Following the methodology of Cooper et al. (2013a) and due to the lack of a North American Vertical Datum of 1988 (NAVD 88) for Hawai‘i, we map mean sea-level values upon the 19-year epoch value of mean higher high water (MHHW) at the Honolulu tide gauge for James Campbell and at the Kahului tide gauge for Kanaha and Keālia to assess flooding at high tide (accessed at tidesandcurrents.noaa.gov). The hypsometric curve depicts the additional area that is flooded (dA) as sea-level is increased in increments of 0.20 m, which approximates the LiDAR vertical uncertainty. Combined with the SLR projection it gives the speed (dA/dt) and acceleration of flooding (d^2A/dt^2).

The critical elevation is identified at the sea-level at which d^2A/dz^2 is a maximum. For a linear rise in sea-level with time, the critical elevation separates flooding into a slow phase (relatively low dA/dt) and a fast phase (relatively high dA/dt). To determine the temporal uncertainty of each flooding phase we create a mixture distribution SLR curve from Vermeer and Rahmstorf’s (2009) B1, A2, and A1FI SLR curves. The B1 (1.04 m by 2100), A2 (1.24 m), and A1FI (1.43 m) economic emission scenarios address how future global sea-level may change under different social, economic, technological, and environmental developments (IPCCC 2007). Assuming each scenario SLR curve is evenly weighted and normally distributed we calculate the total mean ($\mu(t)$) and variance ($\sigma^2(t)$) of the final SLR curve respectively:

$$\mu(t) = \frac{1}{3}\mu_{B1}(t) + \frac{1}{3}\mu_{A2}(t) + \frac{1}{3}\mu_{A1FI}(t) \quad (4)$$

$$\sigma^2(t) = \frac{1}{3}[(\mu_{B1} - \mu(t))^2 + {\sigma_{B1}}^2] + \frac{1}{3}[(\mu_{A2} - \mu(t))^2 + {\sigma_{A2}}^2] + \frac{1}{3}[(\mu_{A1FI} - \mu(t))^2 + {\sigma_{A1FI}}^2] \quad (5)$$

From the SLR curve we calculate the temporal uncertainty of the critical elevation based upon SLR projections alone (σ_{t_s}) and SLR projections and topography ($\sigma_{t_{s+z}}$).

$$\sigma_{t_s} = \frac{\sigma_s(t_T)}{\frac{d\mu_s(t_T)}{dt}} \quad (6)$$

$$\sigma_{t_{s+z}} = \frac{\sqrt{\sigma_s(t_T)^2 + \sigma_z(t_T)^2}}{\frac{d\mu_s(t_T)}{dt}} \quad (7)$$

This analysis allows us to determine whether incorporating hypsometry into management and planning makes a quantifiable difference.

5. Using ranked management concerns to define vulnerability

We present a vulnerability-ranking process to aid in the prioritization of coastal wetland conservation actions in response to SLR. A spatial model and geographic information system (GIS) is used to map vulnerability based upon a number of parameters defined by expert elicitation. The vulnerability-ranking process developed here is flexible and may be refined to accommodate different planning needs, data availability, and expert knowledge in other regions.

Figure 8 outlines the modeling approach used to assess SLR vulnerability. Study sites are identified based upon the biological integrity of managed resources within an area, the existence of experienced and knowledgeable management staff, and the availability of mapable layers such as high resolution topographic data (Figure 8a). We define vulnerability from a management perspective by identifying those parameters that best characterize how SLR will impact decision maker's ability to accomplish mandated goals and objectives (Figure 8b). Elicited expert knowledge and the best available data is used to rank vulnerability parameters for each study site from very high (5) to very low (1) (Figure 8c). A GIS is used to produce a raster of vulnerability values for each input parameter, and a weighted geometric mean is employed to map cumulative vulnerability (Figure 8d-f). If wetland managers accept the designated 'high vulnerability' areas, then vulnerability map products may be used for adaptive management planning (Figure 8g-h). Wetland experts can also modify the model and refine the definition of vulnerability if 'high vulnerability' areas are inadequately represented.

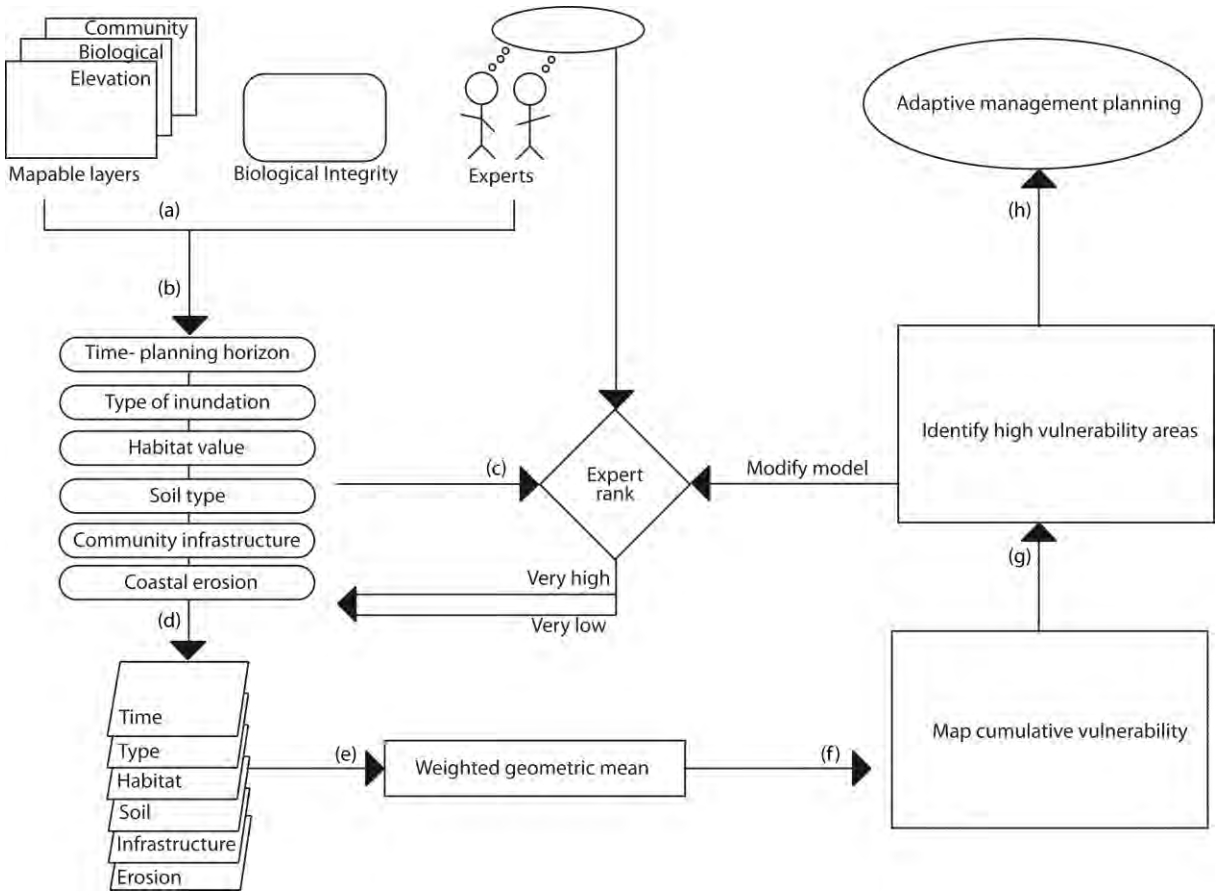

Figure 8. Vulnerability model flow diagram. See text for detailed description.

Once study sites and corresponding on- site experts are identified, coastal wetland and strand vulnerability to SLR is defined by characterizing five input parameters: 1. Type of inundation, 2. Time of inundation, 3. Habitat value, 4. Soil type, and 5. Infrastructure, 6. Coastal erosion. Type of inundation compares wetland manager's ability to manage impacts due to marine inundation (surface flooding from the ocean), and groundwater inundation (associated with rising water tables). Time of inundation assesses wetland manger's planning horizon or their ability to create and employ long-term adaptive management strategies in response to impacts. The habitat value parameter creates an inventory of the emphasis that is placed upon the management of key species within coastal strand, wetland, and upland habitats. Soil type is used to identify poor draining, high salinity, hydric soils that may act as ponding areas for floodwaters. The infrastructure parameter is used to identify regions within the managed bounds that if inundated will also flood surrounding community infrastructure. The coastal erosion parameter models the position of future shorelines under elevated sea-level.

Face-to-face surveys conducted at each study site asked wetland experts to rank their vulnerability to SLR from very low (1) to very high (5) based upon the six input parameters (table 3). Wetland experts are identified as those individuals who from training, research, and personal experience (5-20+ years) possess the greatest capacity to assess how SLR will impact future management strategies. In the case of multiple respondents for each study site, a weighted confidence approach is used such that a greater importance is given to expert rankings made with higher

confidence (Equation 8) (Halpern et al. 2007). Each input parameter and the ranking process are explained in more detail in the following text.

$$VulnerabilityParameter = \frac{\sum VulnerabilityScore \times Confidence}{\sum Confidence} \quad (8)$$

GIS layers for each input parameter are compiled and 2 m horizontal resolution rasters are produced such that each cell represents a corresponding vulnerability rank unique to each study site (Figure 10-21). The final spatial variation of vulnerability for each study area is found by combining the individual vulnerability parameter rasters using a weighted geometric mean (Equation 2).

$$Final\ Vulnerability = (time^3 \cdot type^3 \cdot habitat^3 \cdot soil^2 \cdot infrastructure \cdot erosion)^{\frac{1}{13}} \quad (9)$$

Weights are assigned to variables to represent their relative importance in determining SLR vulnerability. This approach is mathematically similar to the wetland suitability modeling methodology used by Van Lonkhyzen et al. (2004).

Table 3. Sea-level rise vulnerability for each study area was ranked from very low (1) to very high (5) for each of the six input parameters.

Parameter	Weight		James Campbell	Keālia	Kanaha
Type of inundation	3	Groundwater	5	4	4
		Marine	4	5	4
		Not inundated	1	1	1
Time of inundation	3	2044 (0.3 m)	2	4	3
		2100 (1.0 m)	3	4	5
		Not inundated	1	1	1
Habitat value	3	Coastal strand	4	3	2
		Upland shrub/forest	2	2	3
		Wetlands	5	5	5
Soil type	2	Hydric	3	3	*None
		Non-hydric	1	1	
Infrastructure	1	3 types	4	4	4
		2 types	3	3	3
		1 type	2	2	2
		None	1	1	1
Coastal Erosion	1	Erosion hazard	5	5	5
		No hazard	1	1	1

*The NRCS web soil survey (http://websoilsurvey.nrcs.usda.gov/app/) maps found no hydric soils present at Kanaha.

Areas of marine inundation are identified by isolating DEM cells that are hydrologically connected to the ocean or adjacent flooded cells using the 8-sided method (Cooper et al. 2013a). Inundated areas disconnected from the ocean are assumed to be flooded by rising groundwater levels

(Rotzoll and Fletcher 2013). Wetland experts ranked the vulnerability of their study area to both types of inundation by considering natural and constructed features that may impede surface inundation, as well as their dependency upon groundwater sources to maintain pond water levels.

The time of inundation parameter ranks wetland managers ability to implement strategies to manage 0.3 m of SLR by 2040, and 1.0 m of SLR by 2100. Sea-level heights are correlated with time using Vermeer and Rahmstorf (2009) SLR model under the B1 and A1FI scenarios. A very low ability to plan for a specific time period corresponds to a very high vulnerability to SLR. Methodology may be updated to employ new SLR models as global and regional projections improve.

To assess the percent probability that a location is inundated at a particular time we used the cumulative percent probability method mentioned previously to account for the uncertainty of SLR projections and LiDAR data. At each point in the low confidence area for a particular time the probability of flooding is 50%, and at each point in the high confidence area the probability of flooding is 80%. The high confidence area is thus a subset of the low confidence area.

The presence of hydric soils is one of the primary indicators used to identify the occurrence of historical wetlands, as well as potential areas to support the establishment of future wetland ecosystems (Richardson and Gatti 1999; Van Lonkhuyzen et al. 2004). Poorly drained and moderately to strongly saline hydric soil types are identified in each study area using soil maps derived from the NRCS web soil survey (http://websoilsurvey.nrcs.usda.gov/app/). Hydric soils included Keālia silt loam, Kaloko clay, Keaau clay, and Pearl Harbor clay. Hydric soils were not mapped at Kanaha. We assumed that hydric soils are more vulnerable than non-hydric soils to prolonged flooding.

Coastal strand, wetland, and upland habitats were mapped at each study site and wetland experts were asked to rank the emphasis that is placed upon the management of the corresponding wildlife. Managed areas that have a very high habitat value were ranked very highly vulnerable to SLR. The coastal strand serves as important nesting sites for sea turtles (Fuentes et al. 2010), resting areas for monk seals (Baker et al. 2006), and winter staging sites for migrant shorebirds (Galbraith et al. 2002). In addition coastal dune plants stabilize dunes and if lost will lead to an increase in erosion (Feagin et al. 2005). Wetland areas were delineated by the National Wetlands Inventory (http://www.fws.gov/wetlands/Data/Mapper.html). Wetlands are managed primarily to provide habitat for Hawaiʻi's four endemic and endangered waterbirds. Upland habitats were defined as the non-wetland or coastal strand area and for the most part are not intensively managed.

In addition to managing for biodiversity, coastal and wetland managers also have a commitment to manage upland flood impacts upon both refuge and surrounding community infrastructure. The State of Hawaiʻi Office of Planning provided maps of roads, and urban areas, which are defined by the 2010 U.S. census designated as areas with a population of 2,500 people or more (http://planning.hawaii.gov/gis/download-gis-data/). The National Oceanic and Atmospheric Administration (NOAA) Coastal Change Analysis Program (CCAP) provided regional land cover data that was used to identify developed open space (e.g. golf courses, and rural house lots), cultivated land (e.g. agriculture, and aquaculture facilities), and impervious surfaces (e.g. houses, and buildings)

(http://www.csc.noaa.gov/digitalcoast/data/ ccapregional). The three GIS layers were overlaid and the number of infrastructure types occupied within a 50 m buffer raster cell was tallied. As the number of infrastructure types increases, vulnerability of that area increases and wetland migration is inhibited. This leads to a greater chance that flooding will impact nearby development.

SLR threatens Hawai'i's beaches and dunes with chronic erosion. We modeled the effects of accelerated SLR on the study areas using a hybrid model that combines the change in shoreline predictions due to future sea-level predicted by the Bruun rule, with historical shoreline change data as collected by the University of Hawai'i Coastal Geology Group (http://www.soest.hawaii.edu/coasts/erosion/). We created erosion hazard zones by mapping a polygon that encompassed the area occupied between the current shoreline and the future shoreline position predicted under a 1.04 m and 1.43 m rise in sea-level. Areas occupied within the erosion hazard zone are ranked very highly vulnerable to sea-level rise.

D. PROJECT RESULTS:

1. Characterizing the rate of flooding

1.1. Defining a critical elevation

We identify a critical elevation that separates flooding into a slow and fast phase based upon the local topography of three coastal wetlands. The critical elevation of Keālia is defined at 0.2 m and is predicted to be exceeded by the year 2028 $\pm$ 25 years (Figure 9). Kanaha and James Campbell study areas are located at a slightly higher elevation resulting in a critical elevation of 0.6 m by 2066 $\pm$ 16 years.

We acknowledge that the timeframe of exceedance for the critical elevation is quite large and is mostly a reflection of the quality of currently available data. To determine the critical elevation we deal with two sources of uncertainty; the uncertainty of the SLR model used to correlate sea-level with time, and the uncertainty of the LiDAR data used to identify and map the critical elevation. The large LiDAR uncertainty proves to be a major limiting factor. In comparison to considering SLR model uncertainty alone, accounting for the joint uncertainty of both datasets increases the temporal component of the critical elevation from $\pm$ 5 years to $\pm$ 25 years at Keālia and $\pm$ 9 years to $\pm$ 16 years at James Campbell and Kanaha. As SLR projections and topographic datasets improve, the methods used in this study can be employed with greater confidence.

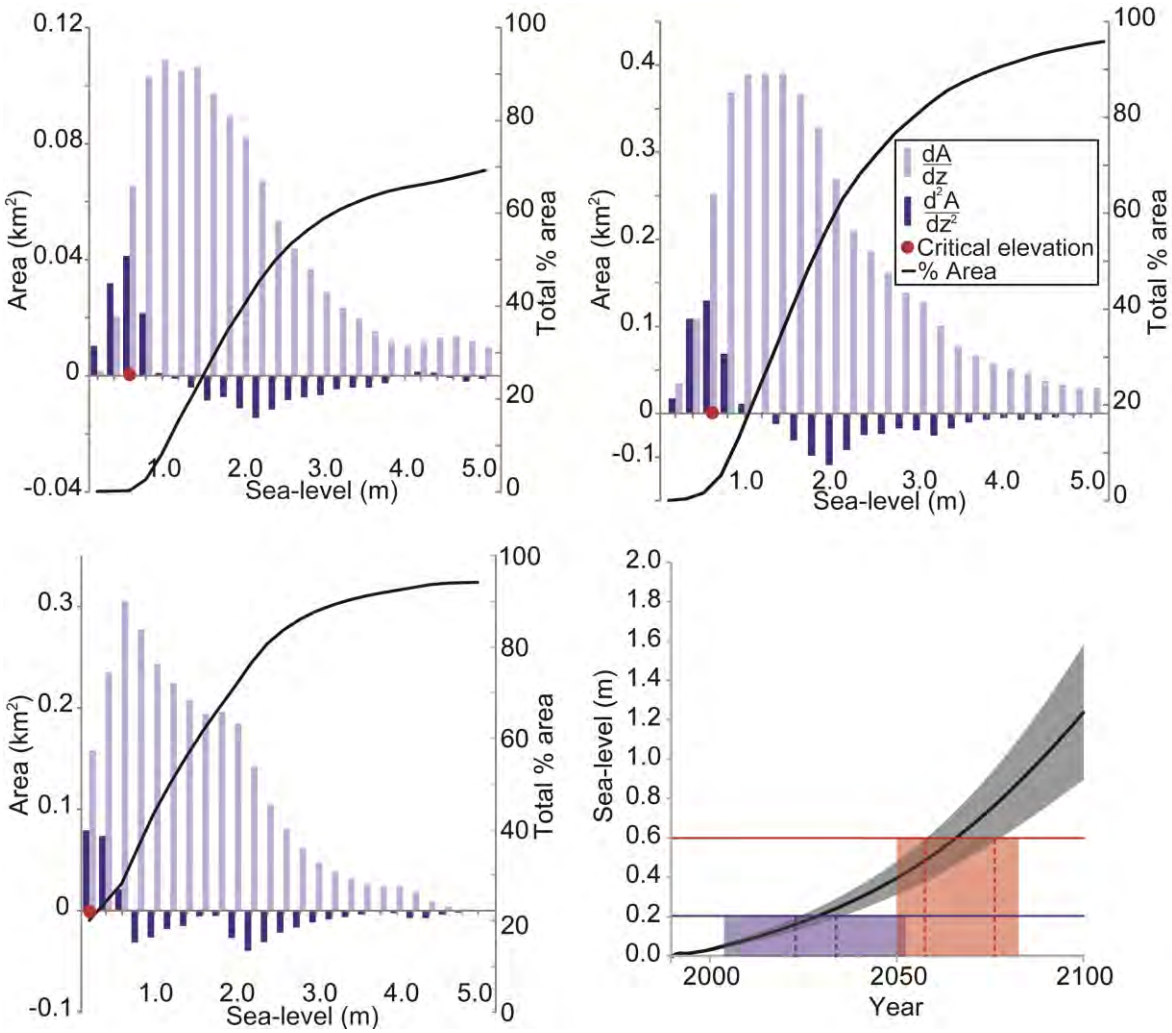

Figure 9. Land area hypsometric curves at **a**, Kanaha, **b**, James Campbell, and **c**, Keālia. The x-axis represents elevation (m) above MHHW. The y-axes represent total percent area at or below a corresponding sea-level value, and area (km^2) inundated as sea-level rises in 0.2 m increments. Temporal uncertainty of the critical elevation is depicted in **d**, based upon the uncertainty of SLR projections alone (dashed lines) and the joint uncertainty of SLR projections and topography (shaded region).

1.2. Mapping SLR impacts for slow and fast phases of flooding

Here we find the slow phase of flooding is defined from present to 2028 ± 25 years (critical elevation = 0.2 m) at Keālia, and from present to 2066 ± 16 years (0.6 m) at Kanaha and James Campbell. To assist decision makers in prioritizing SLR impacts we map flooded areas of high (80%), moderate (50%), and low (2.5%) risk based upon the percent probability that an area will be flooded by sea-level. Due to the similarity of SLR curves during the slow phase, all three economic scenarios agree that there is a moderate risk of 24.1% of Keālia, 2.8% of Kanaha, and 4.3% of James Campbell being flooded (Table 4; Figure 22-24). High and low risk areas encompass 21.0-34.1% of Keālia respectively, 0.3- 17.7% of Kanaha, and 1.7-15.4% of James Campbell. The slow phase of flooding represents the onset of vulnerability as SLR increases coastal erosion, and the extent and frequency of storm surges. Although

initial percent area impacts may appear small, threatened areas include majority of the coastline, and inland wetland environments at James Campbell and Keālia.

Table 4. Percent area of land vulnerable to high, low, and moderate risk for the slow and fast phase of flooding.

Study Area	Flooding Phase	Scenario	Sea-level (m)	% Area High risk	Moderate risk	Low risk
James Campbell	Slow	B1, A1FI	0.60	1.7	4.3	15.4
	Fast	B1	1.04	7.6	14.3	33.5
		A1FI	1.43	15.9	25.9	46.3
Kanaha	Slow	B1, A1FI	0.60	0.3	2.8	17.7
	Fast	B1	1.04	7.0	16.4	36.2
		A1FI	1.43	18.2	28.8	49.6
Keālia	Slow	B1, A1FI	0.20	21.0	24.1	34.1
	Fast	B1	1.04	42.7	51.3	67.6
		A1FI	1.43	53.3	62.2	80.2

The fast phase of flooding represents a time in which the bulk of impacts due to SLR are predicted to occur. We define the fast phase of flooding from 2028 $\pm$ 25 years to 2100 at Keālia and 2066 $\pm$ 16 years to 2100 at Kanaha and James Campbell. The uncertainty values indicate that in the worst case events the critical elevation of SLR may occur sooner than anticipated allowing for less than 15 years on south Maui, and less than 40 years on North Maui and Oʻahu to conceive, develop, and implement adaptation strategies that meet the challenges of SLR in advance of the largest impacts.

We do not consider the post-21st Century extent of the fast phase as indicated by the hypsometric curve because our SLR model does not exceed the year 2100. At 1.04 m (B1) of SLR there is moderate risk of flooding for 51.3 % of Keālia, 16.4% of Kanaha, and 14.3% of James Campbell (Figure 25-27). Under the worst case scenario of 1.43 (A1FI), moderate risk of flooding impacts increase to 62.2 % of Keālia, 28.8% of Kanaha, and 25.9% of James Campbell (Figure 28-30). SLR impacts experienced along the beaches during the slow phase expand and encroach into the upland vegetation and inland wetlands during the fast phase of flooding. At all 3 study areas, nearly all of the wetlands are subjected to moderate or low risk of flooding.

2. Using ranked management concerns to define vulnerability

Six input parameters; type of inundation, time of inundation, soil type, habitat value, infrastructure, and coastal erosion were used to rank the vulnerability of each study area to SLR. Ranked vulnerability scores were assigned to each input parameter using the best available data and the expert knowledge of wetland managers (Table 3). One of the key issues for wetland managers is identifying which areas may be impacted by marine (salty) inundation, or groundwater (potentially fresh or brackish) inundation. We found that groundwater inundation represents over 90% of the total inundation Kanaha and James Campbell (Table 5; Figure 10b-21b) due to the sand dunes which act as a natural buffer to the ocean. At however Keālia the dominant source of inundation shifts from groundwater to marine when considering low confidence inundation areas flooded by the best case (B1: 1.04 m) scenario, and all flooding under the worst case (A1FI: 1.43 M) scenario. Breeching of the narrow ocean outlet ditch at Keālia allows marine water to enter the main pond and other interior wetlands.

Table 5. Area inundated by marine and groundwater sources of inundation by 2100.

Type of inundation (1.04 m)					
	inundation type	low confidence (P>50%)		high confidence (P>80%)	
		% area	% 2100 inundation	% area	% 2100 inundation
James Campbell	Groundwater	16.0	69.1	11.3	96.3
	Marine	7.2	30.9	0.4	3.7
Kanaha	Groundwater	38.6	98.5	30.8	98.6
	Marine	0.6	1.5	0.4	1.4
Keālia	Groundwater	0.8	1.7	41.7	97.6
	Marine	50.4	98.3	1.0	2.4
Type of inundation (1.43 m)					
	inundation type	low confidence (P>50%)		high confidence(P>80%)	
		% area	% 2100 inundation	% area	% 2100 inundation
James Campbell	Groundwater	29.7	73.2	17.8	70.2
	Marine	10.9	26.8	7.6	29.8
Kanaha	Groundwater	50.2	96.8	40.4	98.4
	Marine	1.7	3.2	0.6	1.6
Keālia	Groundwater	1.0	1.6	1.0	2.0
	Marine	61.1	98.4	52.3	98.0

Survey questions asked wetland managers to rank their vulnerability to SLR by considering their future ability to manage both marine and groundwater impacts. At James Campbell wetland managers believed it would be more difficult to manage future groundwater flooding especially if they needed to pump wetlands to alleviate increased groundwater inputs. Marine flooding was believed to be more difficult to manage at Keālia. Wetlands at Keālia are already experiencing increased salinity values, and wetland managers are challenged with managing impacts upon waterbirds and vegetation. The wetland manager at Kanaha expressed concerns about groundwater inundation, however both types of flooding were ranked as highly vulnerable.

The ability of highly managed ecosystems to successfully adapt to SLR, lies in the capacity of coastal decision makers to develop and implement long-term adaptive management plans. Wetland managers were asked to consider their ability to manage a 0.3 m (1.0 ft) rise in sea-level by 2040, and a 1.0 m rise in sea-level by 2100. Most long-term conservation plans however are based upon shorter time scales, and wetland experts stated that they do not typically plan beyond 15 years into the future. Our analysis revealed that the bulk of inundation at Keālia and James Campbell (57.4%, and 99.5% of total inundation respectively) is projected to occur after 2040 (2040-2100) under the worst case SLR scenario (Table 6; Figure 10c-21c). This coincides with a time period when wetland managers believe they are most vulnerable to SLR.

At Keālia by the year 2040, a 0.30 m rise in sea-level is believed impact majority of the shoreline, as well as initiate expansion of many of the interior (e.g. main pond, and old aquaculture ponds). Sea-level for the year 2100 is modeled at a best case of 1.04 m and a worst case 1.43 m. Inundation expands along the coast, interior wetlands, and surrounding uplands. At Kanaha areas impacted by 2040 are limited to a few small areas along the coast, however the existing interior wetlands make up majority of the impacted area. Under all scenarios by 2100 nearly the entire beach fronting Kanaha is impacted and flooding begins to expand from the interior wetlands into the surrounding industrial area in the east, as well as the roads that boarder the northern (Amala place) and southern (Hana and Haleakala highway) boundaries. At James Campbell less than 1% of the total study area is impacted by 2040 and majority of this area is represented as small low-lying patches along the coast, and a few interior wetlands (e.g. runway wetlands). By 2100 inundated areas expand at all of the major wetland units, interior upland areas, and the coastal land that fronts the sand dunes.

Table 6. Area inundated by 2040, and 2100.

Time of inundation (B1: 1.04 m by 2100)					
	inundation type	low confidence (P>50%)		high confidence (P>80%)	
		% area	% 2100 inundation	% area	% 2100 inundation
James Campbell	2040 (0.3 m)	0.9	4.1	0.1	1.1
	2100 (1.04 m)	22.3	96.1	11.6	98.9
Kanaha	2040 (0.3 m)	25.2	64.1	25.0	79.8
	2100 (1.04 m)	14.1	35.9	6.3	20.2
Keālia	2040 (0.3 m)	25.7	50.0	22.7	53.1
	2100 (1.04 m)	25.6	50.0	20.0	46.9
Time of inundation (A1FI: 1.43 m by 2100)					
	inundation type	low confidence (P>50%)		high confidence (P>80%)	
		% area	% 2100 inundation	% area	% 2100 inundation
James Campbell	2040 (0.3 m)	0.9	2.3	0.1	0.5
	2100 (1.43 m)	39.6	97.7	25.3	99.5
Kanaha	2040 (0.3 m)	25.2	48.5	25.0	60.8
	2100 (1.43 m)	26.7	51.5	16.1	39.2
Keālia	2040 (0.3 m)	25.7	41.3	22.7	42.6
	2100 (1.43 m)	36.5	58.7	30.6	57.4

Wetland experts assessed the value of the three major habitats based upon the emphasis that is placed upon the management of the corresponding wildlife. Habitats that are highly valued are more vulnerable to SLR because they will require the most time and resources to mitigate SLR impacts. Wetlands were found to be the most important habitats due to the role that they play in the preservation of endangered waterbirds, and were ranked very highly vulnerable to SLR. Coastal strand

habitats ranked second based upon the priority each refuge gives towards the management of native coastal plants, the monk seal, and sea turtles. Upland habitats ranked the lowest and while they may be managed for a few native plants, uplands are largely occupied by overgrown, low lying shrubs.

The percent area of habitat inundated by SLR is summarized in Table 7. Unlike SLAMM we do not model habitat change, therefore rather than using the land coverage types defined by SLAMM (Table 2), we summarized impacts for the coastal strand, wetland, and upland environments. With the exception of James Campbell, under all three scenarios wetlands habitats are predicted to experience the greatest change as sea-level rise increases both wetland area and water depth (Table 7). Keālia and Kanaha coastal strand areas are predicted to experience the greatest impact from sea-level rise alone. Under a 1.04 m rise in sea-level there is a high confidence that 19.7%, 67.2%, and 86.0% of upland areas may become flooded. Upland areas flooded by groundwater inundation may function as future wetland mitigation areas if they are managed properly.

Table 7. Percent area of habitat inundated by sea-level rise.

High confidence (P>80%)									
	James Campbell			Keālia			Kanaha		
Habitat type	**0.3 m**	**1.04 m**	**1.43 m**	**0.3 m**	**1.04 m**	**1.43 m**	**0.3 m**	**1.04 m**	**1.43 m**
Coastal strand	0.4	8.7	19.9	10.5	27.6	36.4	7.5	26.4	39.2
Wetland	0.1	19.7	38.8	37.1	67.2	79.5	75.3	86.0	93.2
Upland	0.0	5.2	14.8	0.3	4.0	12.5	0.1	3.9	28.6
Low confidence (P>50%)									
	James Campbell			Keālia			Kanaha		
Habitat type	**0.3 m**	**1.04 m**	**1.43 m**	**0.3 m**	**1.04 m**	**1.43 m**	**0.3 m**	**1.04 m**	**1.43 m**
Coastal strand	0.4	8.7	19.9	10.5	27.6	36.4	7.5	26.4	51.4
Wetland	0.1	19.7	38.8	37.1	67.2	79.5	75.3	86.0	95.8
Upland	0.0	5.2	14.8	0.3	4.0	12.5	0.1	3.9	29.7

Poor draining, high salinity, hydric soils occupy relatively large areas at James Campbell and Keālia (Figure 10d-21d). The hydric soil layer at these two study areas include not only existing wetlands but surrounding upland areas that may become prone to long periods of standing water in the future due to the presence poorly drained soils. Kahana was the only study area that lacked hydric soils in the NRC soil maps.

On the basis of infrastructure alone, the areas of the highest vulnerability are located near refuge infrastructure or along the refuge boundaries bordered by community infrastructure (Figure 10f-21f). As the number of community infrastructure types increases there is a greater risk that flooding within the refuge will impact bordering roads, urban, and rural communities. The southern region of the Keālia study area occupies the largest number of infrastructure types including North Kihei road, coastal homes, and is within the urban cluster of Kihei, a population based designation assigned by the 2010 census. The southeast region of James Campbell has the greatest number of infrastructure types due to the close proximity to the surrounding Kahuku community, Kamehameha Highway, and the sewage treatment facility. Kanaha is located in downtown Kahului, Maui and is completely surrounded by

development. Accounting for land and building values in Kahului, a 0.75 m rise in sea-level would result in a loss of $57.5 million dollars (Cooper et al. 2013a).

Erosion hazard zones were mapped for a 1.04 and 1.43 m rise in sea-level at all three study areas. The study area beaches are all currently eroding, with the largest historical erosion rate at Kanaha beach Park (-0.35 $\pm$ 0.02 m) (Fletcher et al. 2012). The erosion hazard zones encompass majority of the current beaches. Under both SLR scenarios the erosion hazard zone at Kanaha intersects the sewage treatment plant, and the road located seaward of Kanaha Wildlife Refuge (Amala Pl.). The erosion hazard zone at Kealia also intersects North Kihei road, and the homes located in the eastern portion of the mapped area. At James Campbell coastal erosion may impact the ocean outlet ditches, which are used to reduce flooding in the wetlands and upland environments. At all three study areas infrastructure and coastal erosion were assigned a lower rank and although it was important that we consider their impacts, these two parameters played less of a role in determining the final vulnerability.

Composite vulnerability scores were compiled using a geometric mean and the highest vulnerability areas were mapped for each study area (Figures 31-36). We distinguished between low and high confidence mapped areas based upon the percent probability that an area will inundated by SLR or fall within an erosion hazard zone. High vulnerability areas at each study area can be defined based upon their corresponding ranked input parameters. At Keālia the majority of high vulnerability areas are characterized marine inundated wetlands areas with hydric soils impacted after 2040 and coastal areas that fall within the erosion hazard zones. As mentioned previously Kanaha lacks hydric soils and therefore vulnerability is defined based upon five input parameters. High vulnerability areas at Kanaha are characterized largely by wetland habitats impacted by groundwater inundation. There are a few coastal and upland habitat areas that ranked high vulnerability due to their close proximity to infrastructure, or the threat of coastal erosion. At James Campbell high vulnerability areas are defined as wetland habitats with hydric soils, impacted by groundwater inundation after 2040. High vulnerability areas also include coastal habitats that fall within the erosion hazard zones and a few upland areas flooded by groundwater after 2040.

E. ANALYSIS AND FINDINGS:

1.1. Strategies to manage slow and fast phases of flooding

Hawaiʻi's coastal wetlands are representative of Pacific Island wetlands due to their relatively small size, diversity of endemic and endangered species, and proximity to rapidly increasing human populations that depend upon wetland resources. Impacts associated with SLR exacerbate flooding of nearby coastal communities during storm events, as well as habitat loss, which is widely used as a measurement of the risk of extinction (Iwamura et al. 2013). Globally, resource managers will be challenged to preserve existing habitats through engineering, relocating habitats to higher elevations, and abandoning existing habitats when the magnitude of SLR overwhelms all other efforts.

Using the inundation maps provided in this study, wetland managers can begin prioritizing responses for the slow and rapid phases of SLR. Providing a local critical elevation and a timeframe for the largest impacts of SLR enables wetland managers to begin formulating long-term adaptive management strategies. The methods used here are applied to wetlands in Hawaiʻi, however they are

applicable to all coastal stakeholders interested in managing resources and defining new policies in response to SLR.

Management efforts for the slow phase of flooding should be focused primarily on moderate and high risk of flooding areas at the beaches and coastal strand. SLR is an important factor in historical shoreline change (Romine et al. 2013), and future SLR will likely worsen the long term coastal erosion rates (Fletcher et al. 2013; Zhang et al. 2004). The first organisms to be impacted by SLR include the endangered monk seals that require beaches for resting, and molting (Baker et al. 2006) and the sea turtles that require beaches for nesting (Fuentes and Cinner 2010). Intertidal habitats also serve as important staging sites where migrant shorebirds can feed and rest and the loss of such sites can cause severe 'bottleneck' effects on migratory populations (Iwamura et al. 2013). As sea-level continues to rise, beaches will naturally migrate landwards unless prevented by structures such as roads, home lots, etc. (Fish et al. 2008). Facilitating the cross-shore movement of beach habitats may preserve endangered and threatened organisms. In urban areas like Kanaha this may be more of a challenge.

In addition to managing current impacts of the slow phase of flooding, wetland managers will also be challenged to create future adaptive management strategies to plan for the fast phase of flooding. As SLR transitions into the fast phase, flooding along the beaches will begin to encroach landward as both marine and groundwater elevations rise. To preserve inland wetland habitats, wetlands will need to be pumped more frequently to maintain low water levels preferred by wildlife, and prevent flooding upon surrounding communities. Increased salinity by groundwater intrusion may also cause more salt tolerant vegetation to replace the native plants required by waterbirds for food, foraging, and the construction of nests. Future studies should focus on identifying when and where groundwater inundation will salinize existing and potentially new wetlands.

The timeframe by which intensive management can aid in the preservation of coastal habitats is limited. Wetland mitigation sites will need to be identified both within and potentially outside of current wetland refuge boundaries. Making these decisions, in the context of specific timeframes of vulnerability, may enhance the capacity of stakeholders to create management plans that increase the resiliency of systems and support the ability of natural systems to adapt to change.

2. Using ranked management concerns to define vulnerability

Under changing climate conditions it will be increasingly untenable to achieve all conservation objectives for habitats, species and protected areas (Hossell et al. 2003). The greatest challenge will be prioritizing management actions in response to impacts. A number of studies have developed vulnerability-ranking processes where threats with the greatest impact are generally assigned highest priority and dealt with first (e.g. Fuentes & Cinner 2010; Selkoe et al. 2008; Halpern et al. 2007). This study is unique in that it couples expert knowledge and empirical data to define input parameters that systematically rank SLR vulnerability at a specific area. To date, the majority of insular SLR assessments have focused on global impacts, however there is a need for finer scale analysis because most management happens at a regional or local scale.

The method used here translates the ranking process into a series of maps that identify high vulnerability areas where adaptive management efforts are most needed. Decision makers will feel more confident in focusing resources to manage these areas because of the integral role they played in identifying and ranking each of the input parameters. The entirety of this process should encourage the discussion of how managing high priority or high vulnerability areas will impact current management objectives and goals. Conservation strategies most likely will need to be updated to meet the challenges of future SLR impacts. Management will need to determine which areas can be preserved, relocated or some areas may possibly need to be abandoned. In the case of urban wetlands, high vulnerability flooded areas will require continuous maintenance to alleviate flooding upon the surrounding community.

We acknowledge that various management groups or regions have different goals and objectives. The strength of this approach is that the rankings as well as input parameters and data can be updated and tailored to reflect the needs of the user. For the purpose of this study we focused on the needs of wetland managers. It is important to note that the quality of model output is a function of the quality of input data, and expert knowledge. Vertical error of a DEM has the largest influence on defining areas of inundation (Zhang 2011), and it is recommended that LiDAR data be used by decision makers to most accurately identify areas vulnerable to SLR (Cooper et al. 2013b). By considering the uncertainty of all data sources used in this study we are able to provide decision makers probabilistic estimates (e.g. 80%, 50%) of SLR vulnerability or risk.

The expert knowledge elicitation process greatly benefits from in-person surveys which allows for input parameters to be adequately defined or updated so that they truly are beneficial in determining rank. Our study employed a small sample size of experts due to limited management staff at each study site. Rather than consulting a larger group of experts who may have a general idea of how each coastal ecosystem functions, wetland managers found it more beneficial to sample a smaller number of experts who are extremely familiar with the goals, objectives, and needs of each study area to provide well-functioning habitats.

The greatest gap in knowledge arose when defining long-term plans from the perspective of climate science models and wetland experts. SLR is a relatively slow process, and the majority of impacts are predicted and modeled for the second half of the century. Wetland experts cite the U.S. Fish and Wildlife Service Comprehensive Conservation Plans as the extent of current long-term planning. These documents provide specific management guidance for each national wildlife refuge system over a period of 15 years (e.g. U.S. Fish and Wildlife Service 2011a, 2011b). Wetland experts attributed their limited ability to plan further into the future to the uncertainty in future funding, limited staff coupled with high number of daily responsibilities and the lack of pressure in the past to plan for longer time periods. There is a great need to extend the planning horizon of natural resource managers to ensure that managed ecosystems may successfully respond to SLR impacts.

F. CONCLUSIONS AND RECOMMENDATIONS:

We provide Pacific Island coastal managers with a number of tools to assess vulnerability of assets due to SLR impacts (e.g. inundation mapping, economic, groundwater, and shoreline change

assessment included in the appendix), however the bulk of this study focused on strategies that target local conservation goals and objectives. To assist coastal decision makers in planning beyond their 15-year long-term time frame we characterize the rate of flooding based upon coastal topography to provide decision makers with a locally based time frame to manage the largest impacts of SLR. As time progresses and the fast phase of flooding approaches, the risk associated with delayed decision-making increases. Expanding upon standard methods to define vulnerability based upon elevation alone, we worked with local wetland experts to create a threat-ranking process that defines vulnerability by those parameters that best characterize how SLR will impact decision makers' ability to accomplish mandated goals and objectives. The strength of this approach is that the rankings and input parameters may be updated as new data becomes available, and tailored to reflect the needs of the user.

The SLR vulnerability maps created in this study can be used as a guide to identify threatened areas and initiate decision making that benefits wetland and coastal strand environments, as well as the neighboring community. By assessing the joint uncertainty of both datasets used in this study, wetland managers can refine their definition of threatened areas based upon the probability that an area will be vulnerable to SLR impacts at a particular time. It is important to note that changes in groundwater chemistry, storms, high waves, and unusually high sea-level events will introduce an element of vulnerability that was not included in this study.

Based upon the findings of this study we recommend the following to coastal decision makers:
1. The long-term planning time frame used by coastal managers should be extended and consider a minimum of 1 ft (0.30 m) rise in sea-level by mid century, and 1 m rise in sea-level by 2100, which was depicted in this study through the use of the best case (B1) scenario. If resources are available fine-scale modeling may be employed to determine local sea-level rise critical elevation and characterize flooding into slow and fast phases.

2. When mapping sea-level rise impacts it is important to consider the uncertainty of mapping products used (e.g. vertical uncertainty of LiDAR data), and sea-level rise projections. Uncertainty values can be incorporated into probabilistic estimates that aid in the definition of high and low confidence of flooding areas.

3. Coastal decision makers should begin prioritizing conservation actions in response to climate change. This process includes:

i. Identifying areas that may be impacted by marine and groundwater sources of flooding associated with sea-level rise.
ii. Identifying areas naturally prone to flooding (e.g. depressions in topography, poor draining soils, low lying areas within the immediate vicinity of the coastline, etc.)
iii. Identifying flooded areas that may impact refuge and community infrastructure.
iv. Identifying coastal assets that fall within the erosion hazard zones.

4. Begin creating adaptive management strategies that set immediate management priorities and identify conservation and mitigation responses for areas prone to a 1 foot (0.30 m) rise in sea-level (Figure 10c-21c).

G. OUTREACH:

1. Webinar presentations

A webinar was presented June 21, 2012 at PICCC offices on global and local patterns of sea level change and possible vulnerabilities.

A webinar was presented on August 21, 2012 to the National Park Service during a planning meeting at Kaloko-Honokohau National Historical Park that covered global and local projections for future sea level change and presented maps of potential vulnerability to the local area under management by Park staff.

A webinar presentation was made on September 12th 2012 to the Hawaiʻi Wetland Joint Venture group. We discussed with managers future sea-level rise projections as well as inundation maps that we created for Keālia Pond National Wildlife Refuge and Kanaha Pond State Wildlife Sanctuary.

2. Community Presentations

Results of our project were presented at the Hawaiʻi Wetlands and Waterbirds Workshop on December 18th. Initially we hoped to present our findings prior to submitting the first draft of our final report, however due to the national Federal furlough the meeting was rescheduled to a later date.

A presentation was made at the Hawaiʻi Water Works Conference on November 18, 2012 that presented results of our mapping the groundwater table in Honolulu and possible impacts due to sea level rise.

A poster pertaining to the products of our research was presented at the August 12, 2011 PICCC Open House.

The impacts of climate change upon Hawaiian wetlands was discussed with a group of middle school students at the at the March 2011 Hawaiʻi Nature Center climate change camp.

3. Meetings

We have met the James Campbell National Wildlife Refuge Project leader Dave Ellis, and Wildlife biologist either at their Haleiwa office or at the Refuge itself on three occasions to present intermediate results and solicit their input and reaction on how to improve GIS layers and other data products produced in this study. Products were also exchanged via email, and the University of Hawaiʻi File Drop Service.

On July 31st, 2012 we met with Jeff Burgett (FWS), Melia Lane-Kam (NPS), Stanton Enomoto (NPS), Arik Arakaki (NPS), and Lisa Marrack (UC Berkeley) to discuss the similarities of products and their applications between our wetland research and the alkaline pond research being done by Ms. Marrak.

We met with the steering committee of the Hawaiʻi Wetland Joint Venture on August 15th, 2013 at the PICCC office to share preliminary findings from our research as well as gain insight and feedback.

We consulted and held in person interviews with the refuge leaders and wildlife biologists at each of the three study sites (June 2013). We provided an in depth overview of sea-level rise and potential impacts upon coastal wetlands. We provided managers with intermediate findings of our research and conducted a sea-level rise survey to gain insight in regards to site specific concerns of sea-level rise

impacts. The results from the survey were used in our threat-ranking process to define SLR vulnerability from a wetland managers perspective.

4. Web resources

The Hawai'i Coastal Geology Website (www.soest.hawaii.edu/coasts) provides background information on SLR, shoreline change data for Oahu, Maui, and Kauai, and PDF copies of the peer reviewed publications produced in this study as well as additional coastal geology manuscripts produced by our group.

H. SCIENCE OUTPUTS:

1. The following publications resulted from this study:

*Cooper H M, Chen Q, Fletcher C H and Barbee M 2013 Assessing vulnerability due to sea-level rise in Maui, Hawai'i using LiDAR remote sensing and GIS. *Climatic Change.* (DOI10.1007/s10584-012-0510-9).

*Cooper H M, Chen Q, Fletcher C H, Barbee M 2013 Sea-level rise vulnerability mapping for adaptation decisions using LiDAR DEMs. *Progress in Physical Geography* (DOI: 10.1177/0309133313496835).

* Romine B M, Fletcher C H, Barbee M M, Anderson T R, and Frazier L N 2013 Are beach erosion rates and sea-level rise related in Hawaii? *Global Planetary Change* **108** 149-157.

*Rotzoll K, Fletcher C 2012 Assessment of groundwater inundation as consequences of sea level rise. *Nature Climate Change***.**: 477-481.

Kane H H, Fletcher C H, Frazer N, Barbee, M. (under review) Decision-makers face a "critical elevation" of flooding due to sea-level rise. *Regional Environmental Change*.

Kane H H, Fletcher C H, Frazer N, Barbee, M. (in preparation) Modeling sea-level rise vulnerability of coastal wetlands using ranked management concerns. *Conservation Biology*.

*manuscript available at http://www.soest.hawaii.edu/coasts/publications/

2. Results of this research were presented at the following conferences:

i. Geological Society of America Annual conference (2012, 2013)
ii. American Geophysical Union Annual conference (2012)
iii. Hawaii Conservation Conference (2011)

I. References

Baker JD, Littnan C L, and Johnston D W 2006 Potential effects of sea level rise on the terrestrial habitats of endangered and endemic megafauna in the Northwestern Hawaiian Islands *Endangered Species Research* **2**:21-30.

Bamber J L and Aspinall W P 2013 An expert judgement assessment of future sea level rise from the ice sheets *Nature Climate Change* (doi:10.1038/NCLIMATE1778).

Church J A, and White N J 2011 Sea-Level Rise from the Late 19th to the Early 21st Century. Survey Geophysics **32** 585-602.

Clough Johnathan and Larson E C 2010a Application of the Sea-Level Affecting Marshes Model (SLAMM 6) to James Campbell NWR (Warren, VT: Warren Pinnacle Consulting, Inc).

Clough Johnathan and Larson E C 2010b Application of the Sea-Level Affecting Marshes Model (SLAMM 6) to Kealia Pond NWR (Warren, VT: Warren Pinnacle Consulting, Inc).

Clough J, Park R A, and Fuller R 2010c SLAMM 6 beta Technical Documentation (Warren, VT: Warren Pinnacle Consulting, Inc).

Cooper H M, Chen Q, Fletcher C H, and Barbee M M 2013a Assessing vulnerability due to sea-level rise in Maui, Hawai'i using LiDAR remote sensing and GIS. *Climatic Change* **116** 547-563.

Cooper H M, Fletcher C H, Chen Q and Barbee M M 2013b Sea-level rise vulnerability mapping for adaptation decisions using LiDAR DEMs. *Progress in Physical* **37** 745-766.

Dewberry 2008 LiDAR QAQC Report Hawaii TO12: Molokai, Maui, Lanai Islands March 2008. Dewberry, Fairfax, Virginia

FGDC 1998 Geospatial positioning accuracy standards, Part 3. national Standard for Spatial Data Accuracy. http://www.fgdc.gov/standards/projects/FGDC-standards-projects /accuracy/ part3/index_html. Accessed September 2013.

Feagin R A, Sherman D J, and Grant W E 2005 Coastal erosion, global sea-level rise, and the loss of sand dune plant habitats *Frontiers in Ecology and the Environment* **3** 359-364.

Fletcher C H, Romine B M, Genz A S, Barbee M M, Dyer M, Anderson T R, Lim S C, Vitousek S, Bochicchio C, Richmond B M 2013 National Assessment of Shoreline Change: Historical Shoreline Change in the Hawaiian Islands: U.S. Geological Survey Open-File Report 2011-1051, 55 p. (Also available at http:pubs.usgs.gov/of/2011/1051.).

Fletcher C H 2009. Sea level by the end of the 21st century: A review. *Shore & Beach* 77 (4) 4-12.

Fletcher C, Rooney J, Barbee M, Lim S-C, Richmond B M 2003 Mapping shoreline change using digital orthophotogeometry on Maui, Hawaii *Journal of Coastal Research* **SI38** 106-124.

Fuentes, M M P B, and Cinner J E 2010 Using expert opinion to prioritize impacts of climate change on sea turtles *Journal of Environmental Management* **9** 2511-2518.

Galbraith H, Jones R, Park R, Clough J, Herrod-Julius S, Harrington B, and Page G 2002 Global Climate Change and Sea Level Rise: Potential Losses of Intertidal Habitat for Shorebirds *Waterbirds* **25** 173-183.

Gardner A S, Moholdt G, Cogley J G, Wouters B, Arendt A A, Wahr J, Berthier E, Hock R, Pfeffer W T, Kaser G, Ligtenberg S R M, Bolch T, Sharp M J, Hagen J O, van den Broeke M R, Paul F 2013 A

Reconciled Estimate of Glacier Contributions to Sea Level Rise: 2003 to 2009. *Science* **340** 852-857.

Gesch D B 2009 Analysis of Lidar Elevation Data for Improved Identification and Delineation of Lands Vulnerable to Sea-Level Rise *Journal of Coastal Research* **SI53** 49-58.

Halpern B S, Selkoe K A, Fiorenza M, and Kappel C V 2007 Evaluating and ranking vulnerability of global marine ecosystems to anthropogenic threats *Conservation Biology* **21** 1301-1315.

Hossell J E, Ellis N E, Harley M J, and Hepburn I R 2003 Climate change and nature conservation: Implications for policy and practice in Britain and Ireland *Journal for Nature Conservation* **11** 67-73.

Intergovernmental Panel on Climate Change (IPCC) 2013 Climate Change 2013 *The Physical Science Basis Summary for Policymakers* ed T F Stocker et al. (Switzerland: IPCC, 2013).

Intergovernmental Panel on Climate Change (IPCC) 2007 *The Fourth Assessment Report of the Intergovernmental Panel on Climate Change* ed S Solomon et al. (Cambridge: Cambridge University Press, 2007).

Iwamura T, Possingham H P, Chades I, Minton C, Murray N J, Rogers D I, Treml E A, Fuller R A 2013 Migratory connectivity magnifies consequences of habitat loss from sea-level rise for shorebird populations *Proceedings of the Royal Society Biological Sciences* **280** 1471-2954.

Jevrejeva S, Moore JC, and Grinsted A 2012 Sea level projections to AD2500 with a new generation of climate change scenarios *Global and Planetary Change* **80-81** 14-20.

Kirwan M L and Temmerman S 2009 Coastal marsh response to historical and future sea-level acceleration *Quartenary Science Reviews* **28** 1801-1808.

Kirwan M L, Buntenspergen G R, D'Alpaos Andrea, Morris J T, Mudd S M and Temmerman S 2010 Ecogeomorphic limits to wetlands survival *Geophysical Research Letters* **37** (doi:101029/GL045489).

Meehl G A, Hu A, Tebaldi C, Arblaster J M, Washington W M, Teng H, Sanderson B M, Ault T, Strand W G and White JB 2012 Relative Outcomes of Climate Change Mitigation Related to Global Temperature Versus Sea-Level Rise. *Nature Climate Change* (doi:10.1038/NCLIMATE1529).

Merrifield and Maltrud 2011 Regional sea level trends due to Pacific trade wind intensification *Geophysical Research Letters* **38** (doi:10.1029/2011GL049576).

Mitsova D, Esnard A M, Li Y 2012 Using enhanced dasymetric mapping techniques to improve the spatial accuracy of sea level rise vulnerability assessments *Journal of Coastal Conservation* **16** 355-372.

Moore J G 1987 Subsidence of the Hawaiian Ridge *In* Decker RW, Wright TL and Stauffer PH (Eds) *Volcanism in* Hawai'i United States Geological Survey Professional Paper, pp. 85-100.

Morris J T, Sundareshwar P V, Nietch C T, Kjerfve B and Cahoon D R 2002 Responses of coastal wetlands to rising sea level. *Ecology* **83** 2869–2877.

National Research Council (NRC) 2007 Elevation Data for Floodplain Mapping. The National Academies Press, Wshington, DC.

Nicholls R J 2011 Planning for the Impacts of Sea Level Rise. *Oceanography* **24** 144-157.

Nicholls R J 2004 Coastal flooding and wetland loss in the 21st century: changes under the SRES climate and socio-economic scenarios *Global Environmental Change* **14** 69-86.

National Oceanic Atmospheric Administration (NOAA) 2010 Mapping Inundation Uncertainty. http://csc.noaa.gov/digitalcoast/_/pdf/ElevationMappingConfidence.pdf. Accessed September 2013.

Osgood D T and Brian Sillman. "From Climate Change to Snails" *Human Impacts on Salt Marshes.* Ed. Brian Sillman, Ed. Edwin Grosholz, Ed. Mark Bertness. Berkeley: University of California Press, 2009. 231-283.

Rahmstorf S, Perrette M, Vermeer M 2011 Testing the robustness of semi-empirical sea level projections. *Climate Dynamics* **39** 861-875.

Rahmstorf S 2010 A new view on sea level rise. *Nature Reports Climate Change* **4** 44-45.

Richardson M S, and Gatti R C 1999 Prioritizing wetland restoration activity within a Wisconsin watershed using GIS modeling. *Journal of Soil and Water Conservation* **54** 537-542.

Rignot E, Velicogna I, van den Broeke M R, Monoghan A, and Lenaerts J T M 2011 Acceleration of the contribution of the Greenland and Antarctic ice sheets to sea level rise. *Geophysical Research Letters* **38** (doi:10.1029/2011GL046583).

Romine B M, Fletcher C H, Barbee M M, Anderson T R, and Frazier L N 2013 Are beach erosion rates and sea-level rise related in Hawaii? *Global Planetary Change* **108** 149-157.

Rotzoll K and Fletcher C 2012 Assessment of groundwater inundation by sea level rise *Nature Climate Change* **3** 477-481

Sallenger A H, Doran K S and Howd P A 2012 Hotspot of accelerated sea-level rise on the Atlantic coast of North America *Nature Climate Change* **2** 884-888.

Selkoe K A, Halpern B S, and Toonen R J 2008 Evaluating anthropogenic threats to Northwestern Hawaiian Islands. Aquatic Conservation: *Marine and Freshwater Ecosystems* **18** 1149-1165.

Slangen A B A, Katsman C A, van de Wal R S W, Vemeersen L L A and Riva R E M 2012 Towards regional projections of the 21st century sea-level change based on IPCC SRES scenarios *Climatic Dynamics* **38** 1191-1209.

Spada G, Bamber J L and Hurkmans R T W L 2013 The gravitationally consistent sea-level fingerprint of future terrestrial ice lost *Geophysical Research Letters* **40** 1-5 (doi:10.1029/2012GL05300).

Stevenson, J C and Kearney M S 2009 Impacts of global climate change and sea-level rise on tidal wetlands. pp. 171-206, in B R Silliman, E D Grosholtz and M D Bertness (eds) *Human Impacts on Salt Marshes: A Global Perspective*. University of California Press: Berkeley, CA.

Tebaldi C, Strauss B H and Zervas C E 2012 Modelling sea level rise impacts on storm surges along US coasts *Environmental Research Letters* **7** 014032.

U.S. Fish & Wildlife Service (USFWS) 2011a *James Campbell National Wildlife Refuge Comprehensive Conservation Plan and Environmental Assessment* (Honolulu, HI: U.S. Fish and Wildlife Service).

U.S. Fish & Wildlife Service (USFWS) 2011b *Kealia Pond National Wildlife Refuge Draft Comprehensive Conservation Plan and Environmental Assessment* (Kihei, HI: U.S. Fish and Wildlife Service).

Van Lonkhuyzen R A, Lagory K E, and Kuiper J A 2004 Modeling the Suitability of Potential Wetland Mitigation Sites with a Geographic Information System *Environmental Management* **33**:368-375.

Vermeer M, Rahmstorf S, Kemp A and Horton B 2012 On the difference between two semi-empirical sea-level models for the last two millennia *Climate of the Past Discussions* **8** 3551-3581.

Vermeer M and Rahmstorf S 2009 Global sea level linked to global temperature *Proceedings of the National Academies of Sciences* USA **106** 21527-32.

Webb E L, Friess D A, Krauss, K W, Cahoon, D R and Guntenspergen G R 2013 A global standard for monitoring coastal wetland vulnerability to accelerated sea-level rise *Nature Climate Change* (DOI 10.1038/NCLIMATE1756).

Zhang K 2011 Analysis of non-linear inundation from sea-level rise using LIDAR data: a case study for South Florida *Climatic Change* **106** 537-565.

Zhang K, Dittmar J, Ross M, Bergh C 2011 Assessment of sea level rise impacts on human population and real property in the Florida Keys *Climatic Change* **107** 129-146.

4. Appendix

A. Vulnerability maps using ranked management concerns

Improving upon standard inundation mapping techniques we develop a ranking system that models sea-level rise (SLR) vulnerability as a function of six input parameters defined by wetland experts: 1. type of inundation, 2. time of inundation, 3. soil type, 4. habitat importance, 5. infrastructure, and 6. coastal erosion. Figures 10-21 map the ranked input parameters for Keālia National Wildlife Refuge (south Maui), Kanaha State Wildlife Sanctuary (north Maui), and James Campbell National Wildlife Refuge (north Oʻahu). Areas flooded by SLR are mapped at low (50% probability of flooding) and high confidence (80%).

Final vulnerability is obtained by calculating the weighted geometric mean of the input vulnerability scores (Figures 31-36). High (80%) and low (50%) confidence areas determined based upon the percent probability of flooding due to SLR. We consider the B1 (1.04 m by 2100) and A1FI (1.43) SLR scenarios.

Areas with the highest composite vulnerability scores are characterized by wetland habitats with hydric soils, impacted by groundwater inundation after 2040. The tools developed in this study can be used as a guide to prioritize conservation actions and initiate decisions to adaptively manage SLR impacts. High vulnerability areas at Keālia are defined as marine inundated wetlands with hydric soils impacted after 2040. Kanaha lacks hydric soils and therefore vulnerability is defined as wetland habitats impacted by groundwater inundation after 2040. At James Campbell high vulnerability areas are defined as wetland habitats with hydric soils, impacted by groundwater inundation after 2040.

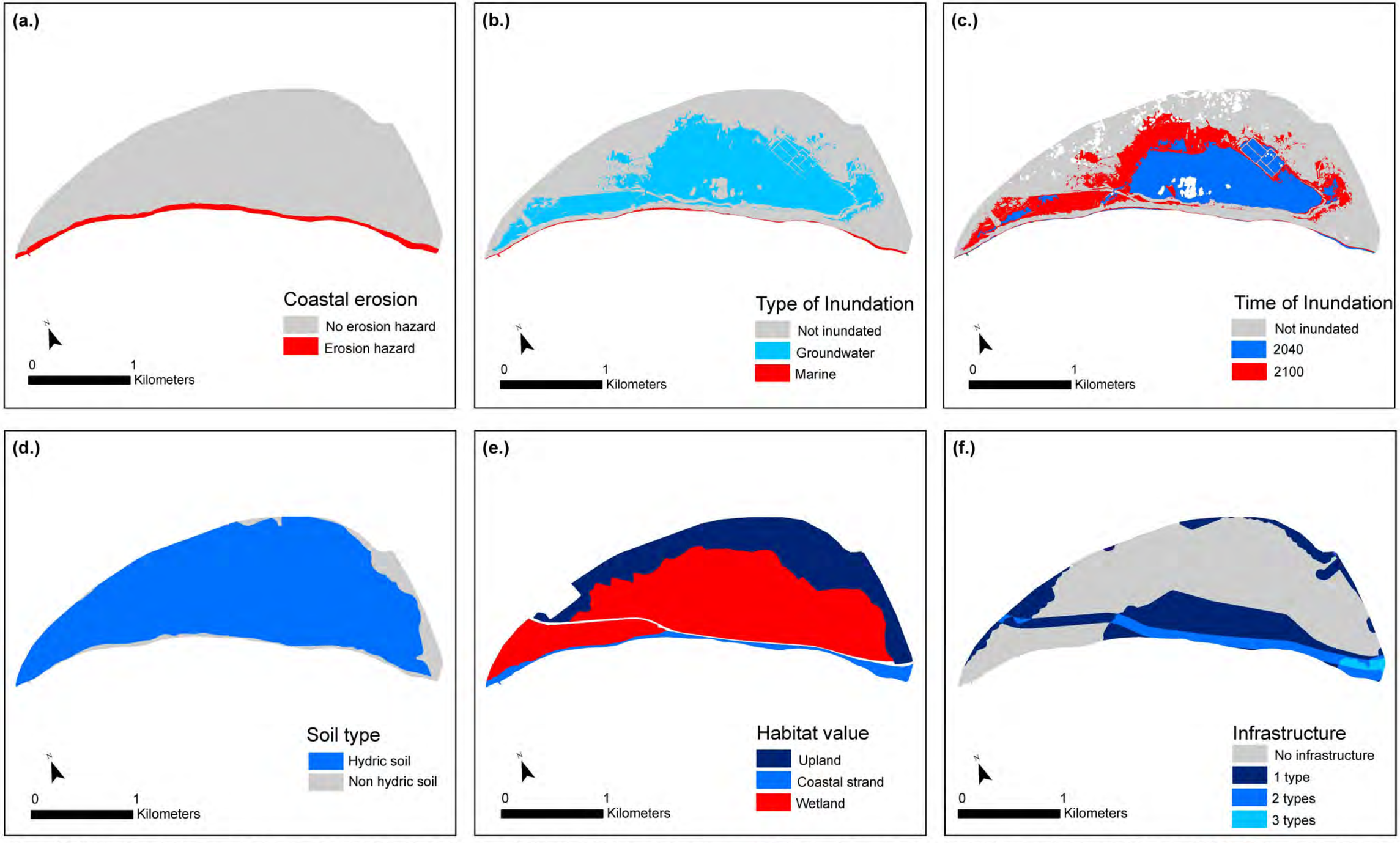

Figure 10. SLR vulnerability maps for Keālia considering high confidence (80% probability) inundation areas under the best case scenario (B1: 0.30 m by 2040 and 1.04 m by 2100). Vulnerability at Keālia is defined by six input parameters; coastal erosion (a) inundation type (b), time of inundation (c), soil type (d), habitat value (e), and infrastructure (f).

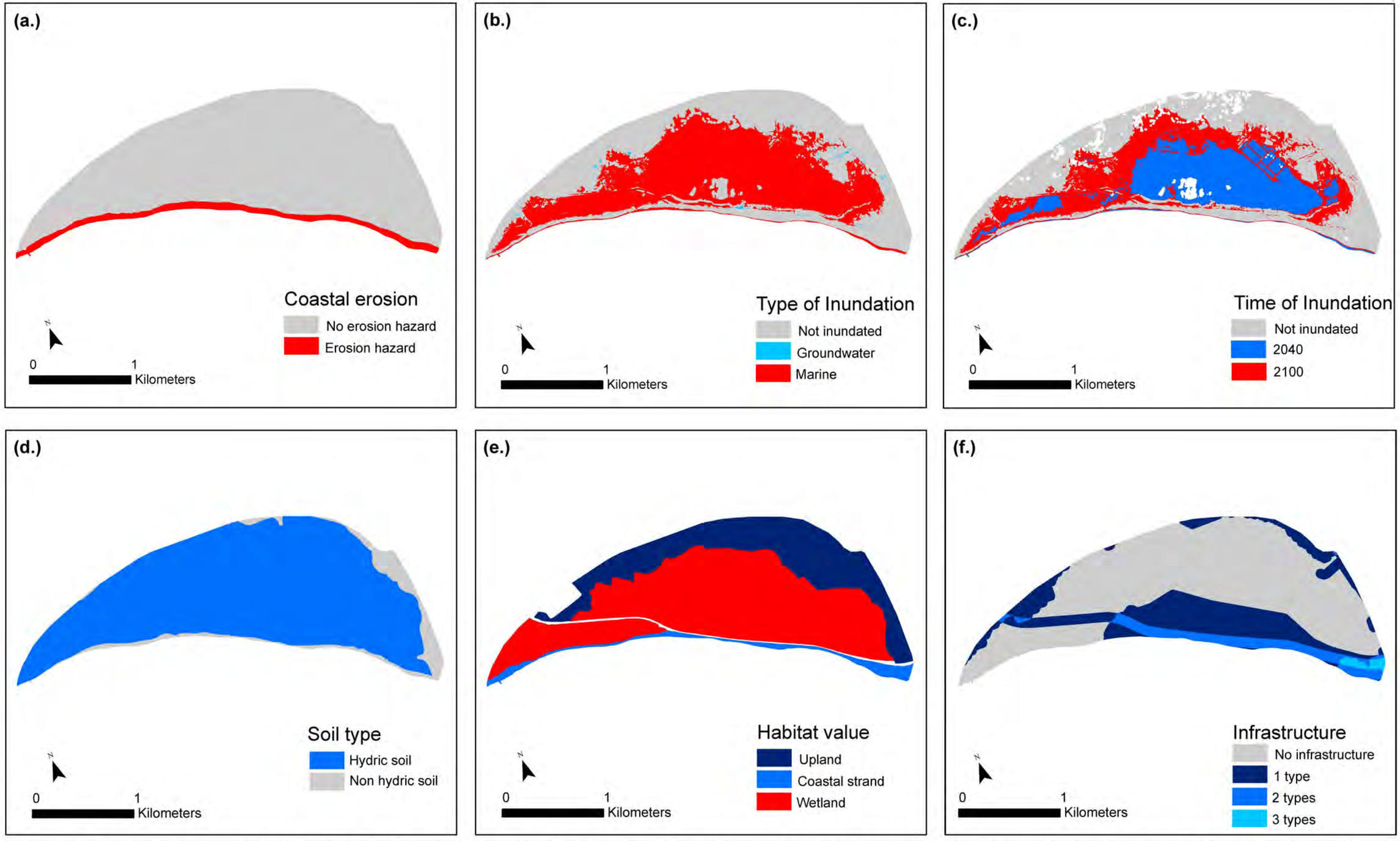

Figure 11. SLR vulnerability maps for Keālia considering low confidence (50% probability) inundation areas under the best case scenario (B1: 0.30 m by 2040 and 1.04 m by 2100). Vulnerability at Keālia is defined by six input parameters; coastal erosion (a), inundation type (b), time of inundation (c), soil type (d), habitat value (e), and infrastructure (f). The dominant source of inundation transitions from groundwater to marine when considering low confidence inundation areas under the best case scenario.

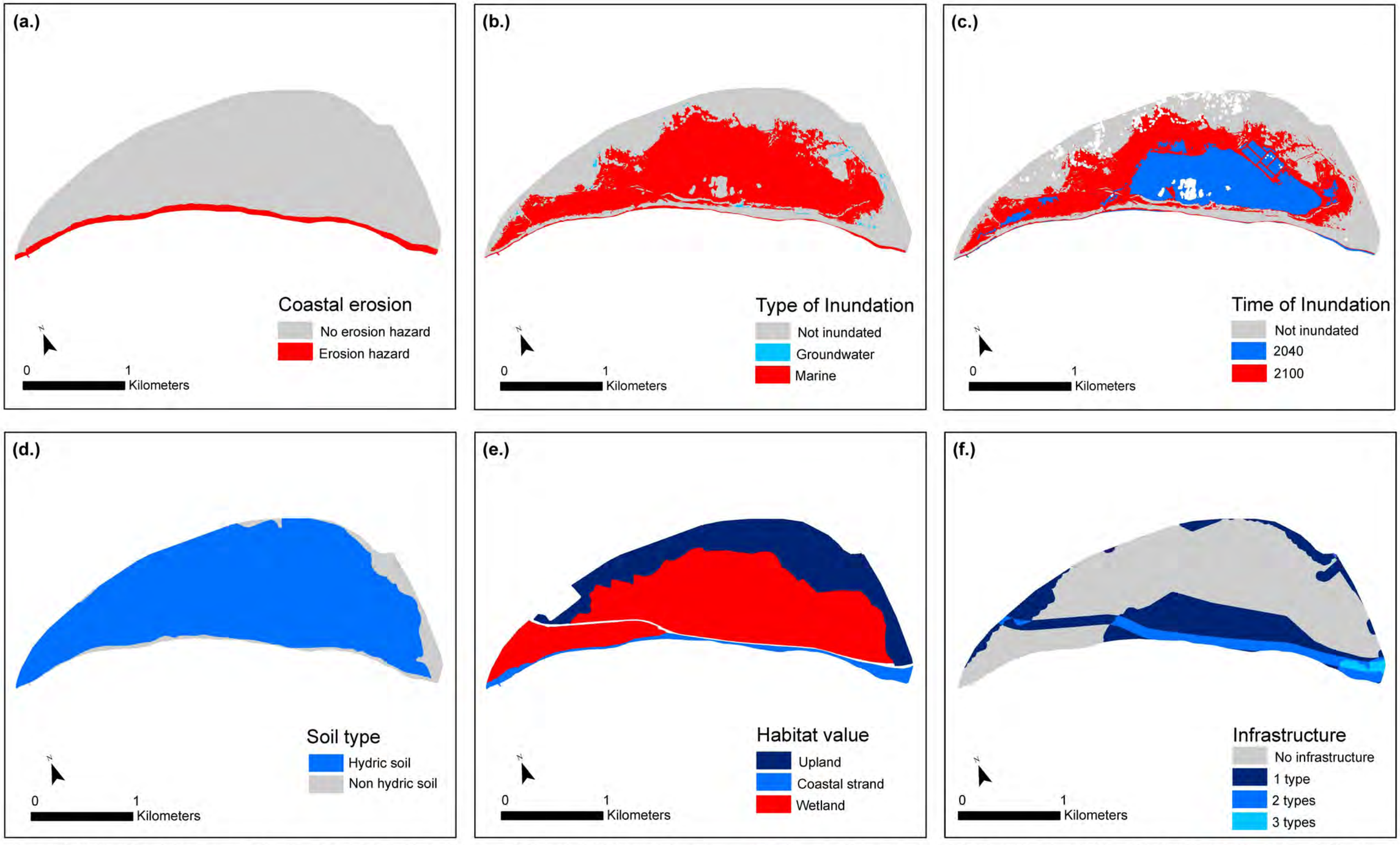

Figure 12. SLR vulnerability maps for Keālia considering high confidence (80% probability) inundation areas under the worst case scenario (A1FI: 0.30 m by 2040 and 1.43 m by 2100). Vulnerability at Keālia is defined by six input parameters; coastal erosion (a), inundation type (b), time of inundation (c), soil type (d), habitat value (e), and infrastructure (f).

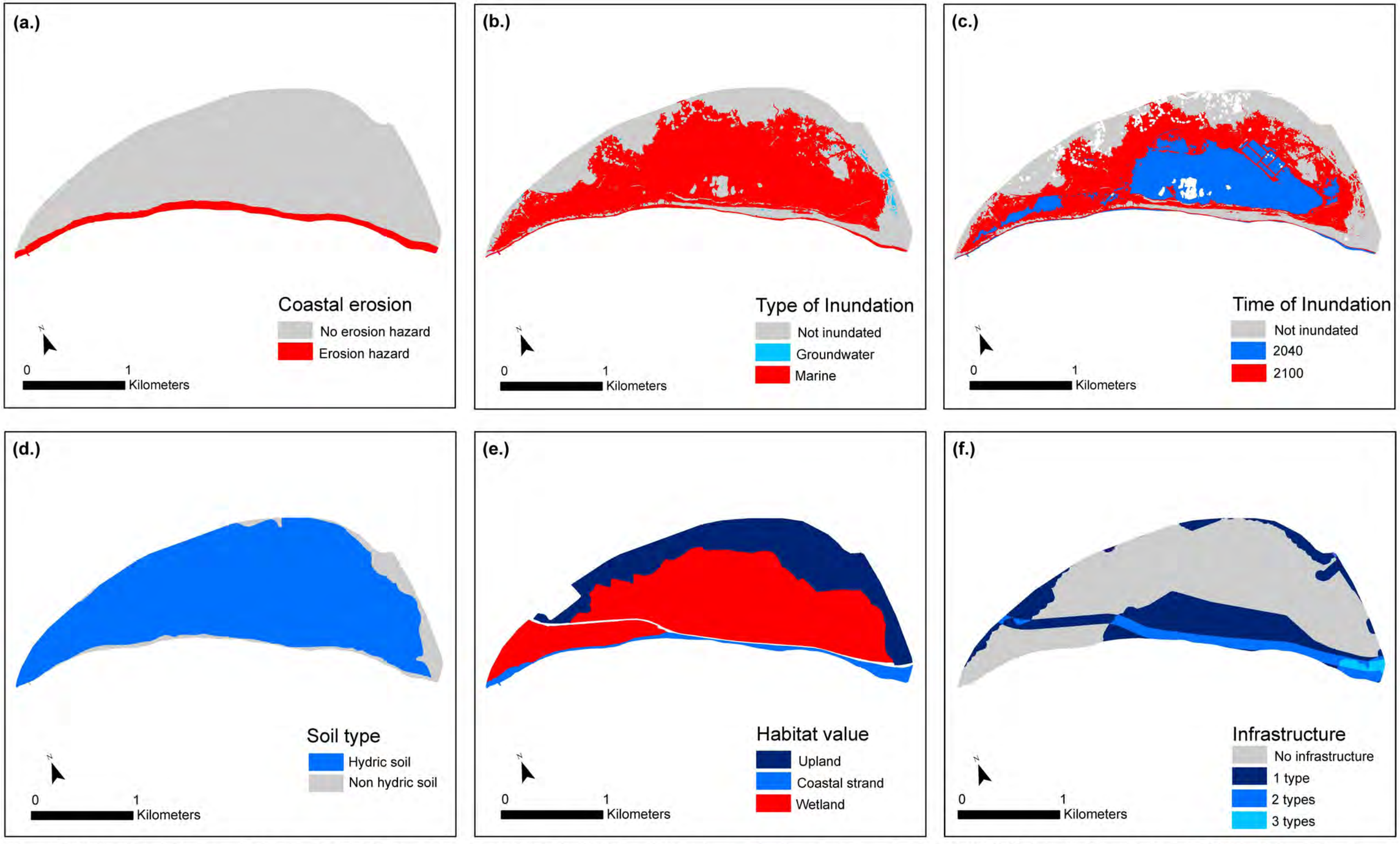

Figure 13. SLR vulnerability maps for Keālia considering low confidence (50% probability) inundation areas under the worst case scenario (A1FI: 0.30 m by 2040 and 1.43 m by 2100). Vulnerability at Keālia is defined by six input parameters; coastal erosion (a), inundation type (b), time of inundation (c), soil type (d), habitat value (e), and infrastructure (f).

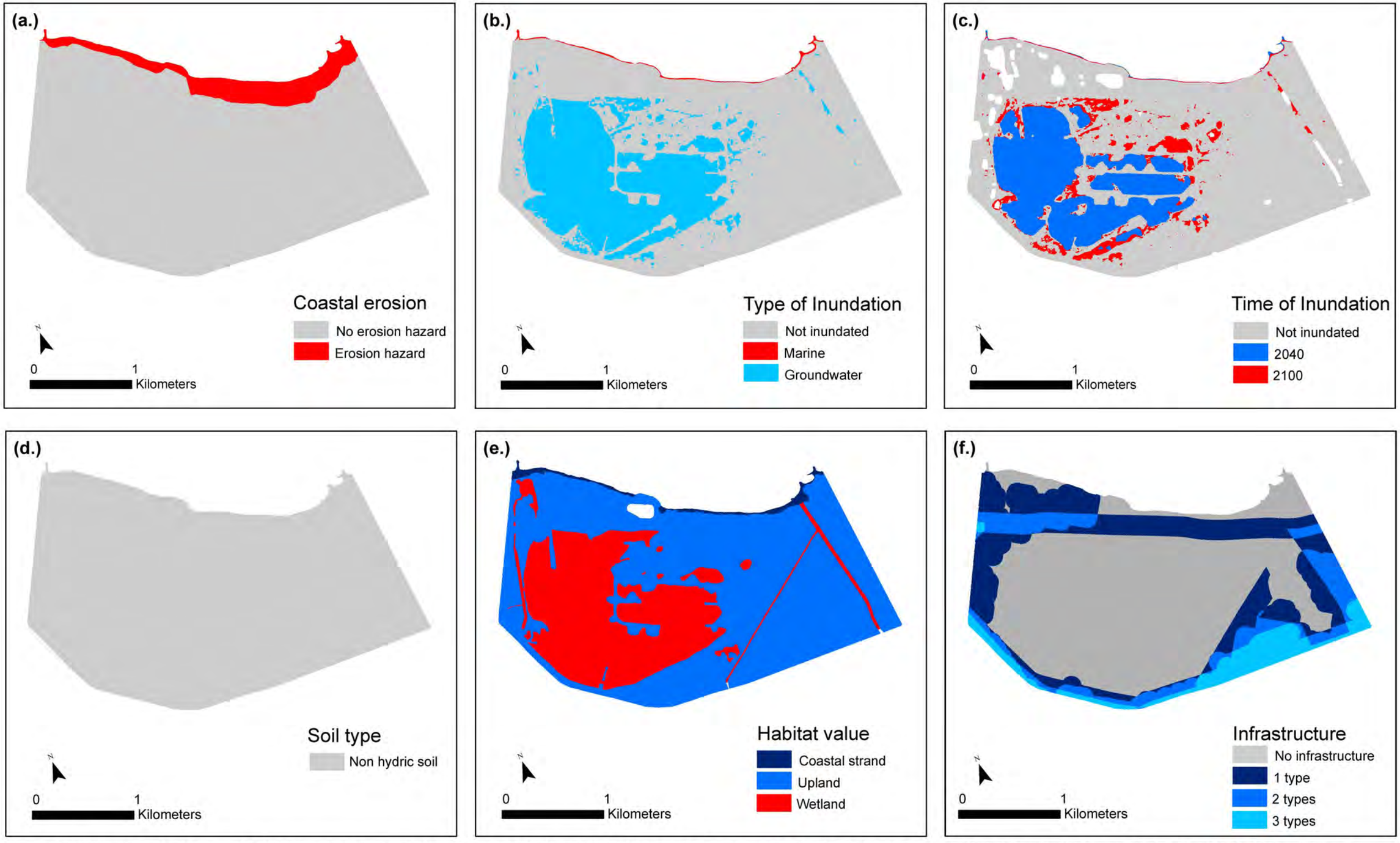

Figure 14. SLR vulnerability maps for Kanaha considering high confidence (80% probability) inundation areas under the best case scenario (B1: 0.30 m by 2040 and 1.04 m by 2100). Vulnerability at Kanaha is defined by five input parameters; coastal erosion (a), inundation type (b), time of inundation (c), habitat value (e), and infrastructure (f). Hydric soils (d) are not present on the NRCS soil maps and could not be used to define vulnerability.

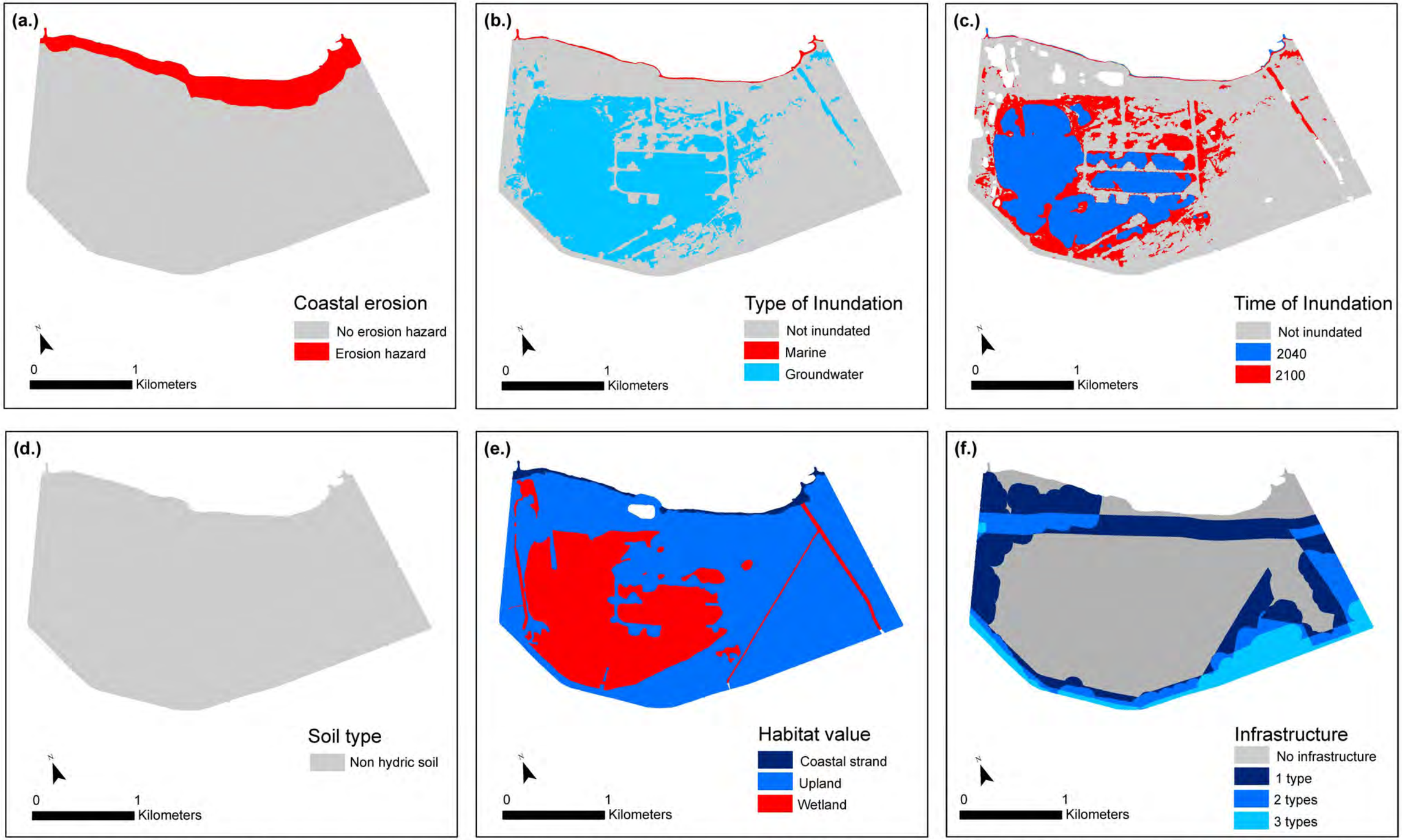

Figure 15. SLR vulnerability maps for Kanaha considering low confidence (50% probability) inundation areas under the best case scenario (B1: 0.30 m by 2040 and 1.04 m by 2100). Vulnerability at Kanaha is defined by five input parameters; coastal erosion (a), inundation type (b), time of inundation (c), habitat value (e), and infrastructure (f). Hydric soils (d) are not present on the NRCS soil maps and could not be used to define vulnerability.

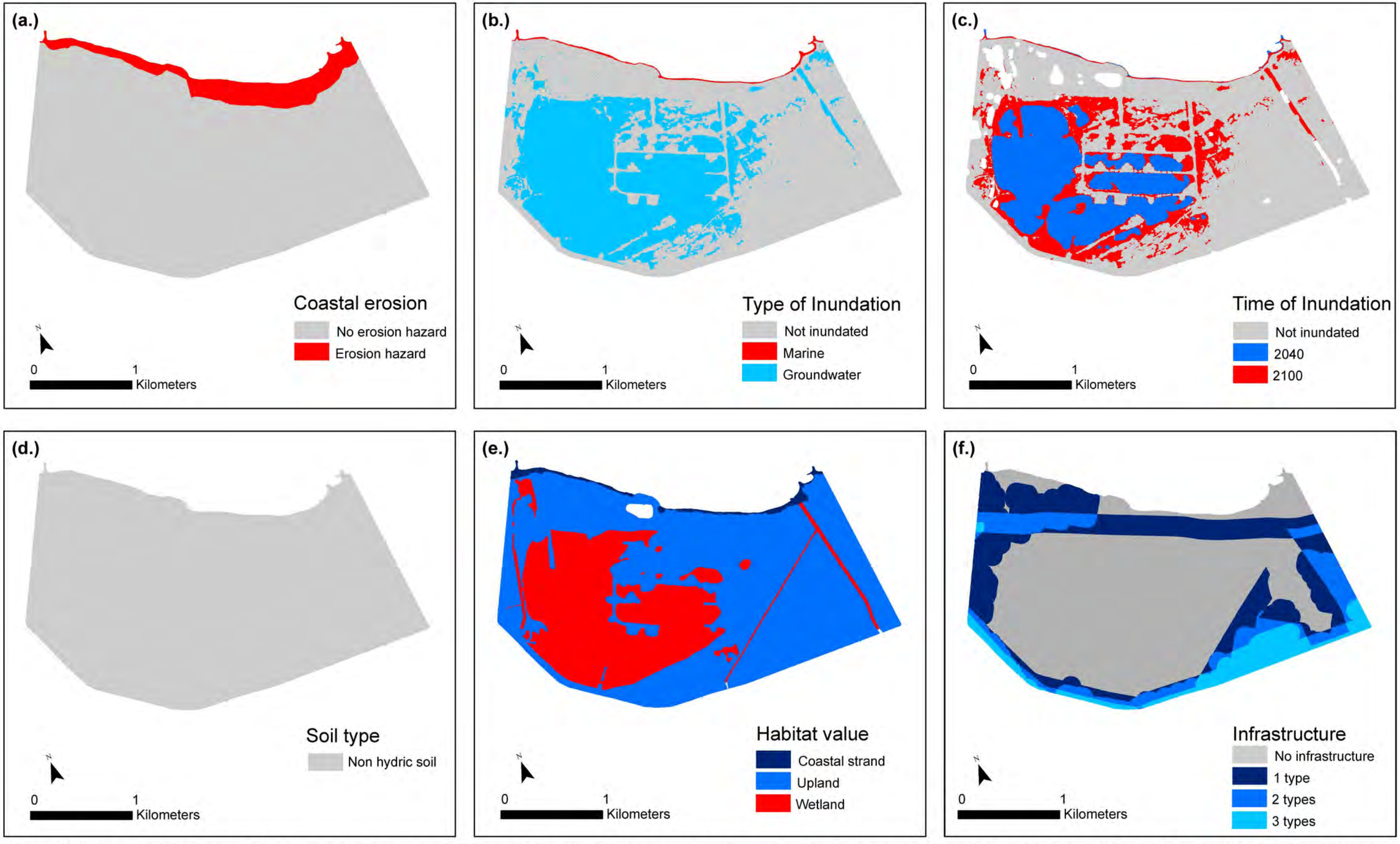

Figure 16. SLR vulnerability maps for Kanaha considering high confidence (80% probability) inundation areas under the worst case scenario (A1FI: 0.30 m by 2040 and 1.43 m by 2100). Vulnerability at Kanaha is defined by five input parameters; coastal erosion (a), inundation type (b), time of inundation (c), habitat value (e), and infrastructure (f). Hydric soils (d) are not present on the NRCS soil maps and could not be used to define vulnerability.

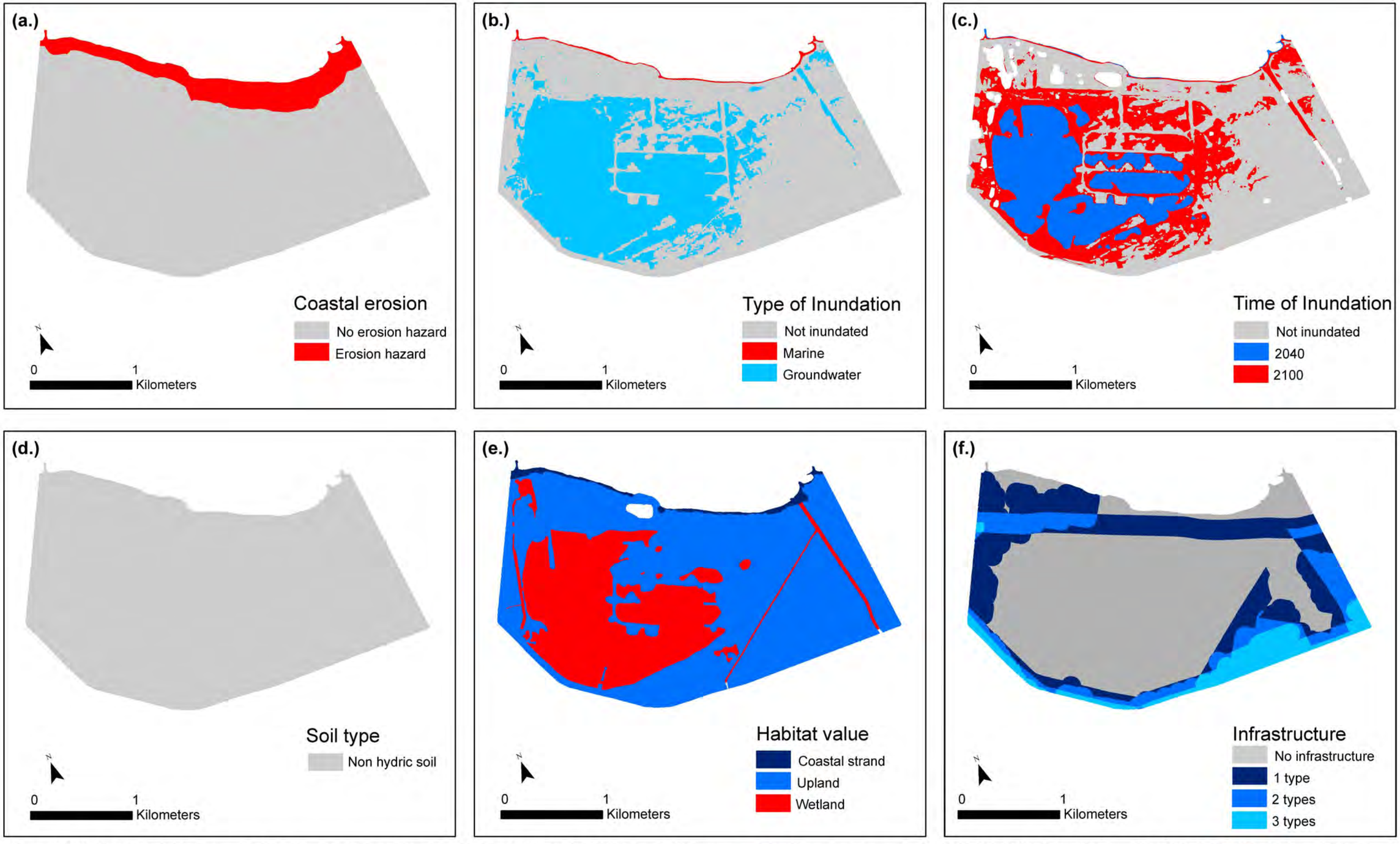

Figure 17. SLR vulnerability maps for Kanaha considering low confidence (50% probability) inundation areas under the worst case scenario (A1FI: 0.30 m by 2040 and 1.43 m by 2100). Vulnerability at Kanaha is defined by five input parameters; coastal erosion (a), inundation type (b), time of inundation (c), habitat value (e), and infrastructure (f). Hydric soils (d) are not present on the NRCS soil maps and could not be used to define vulnerability.

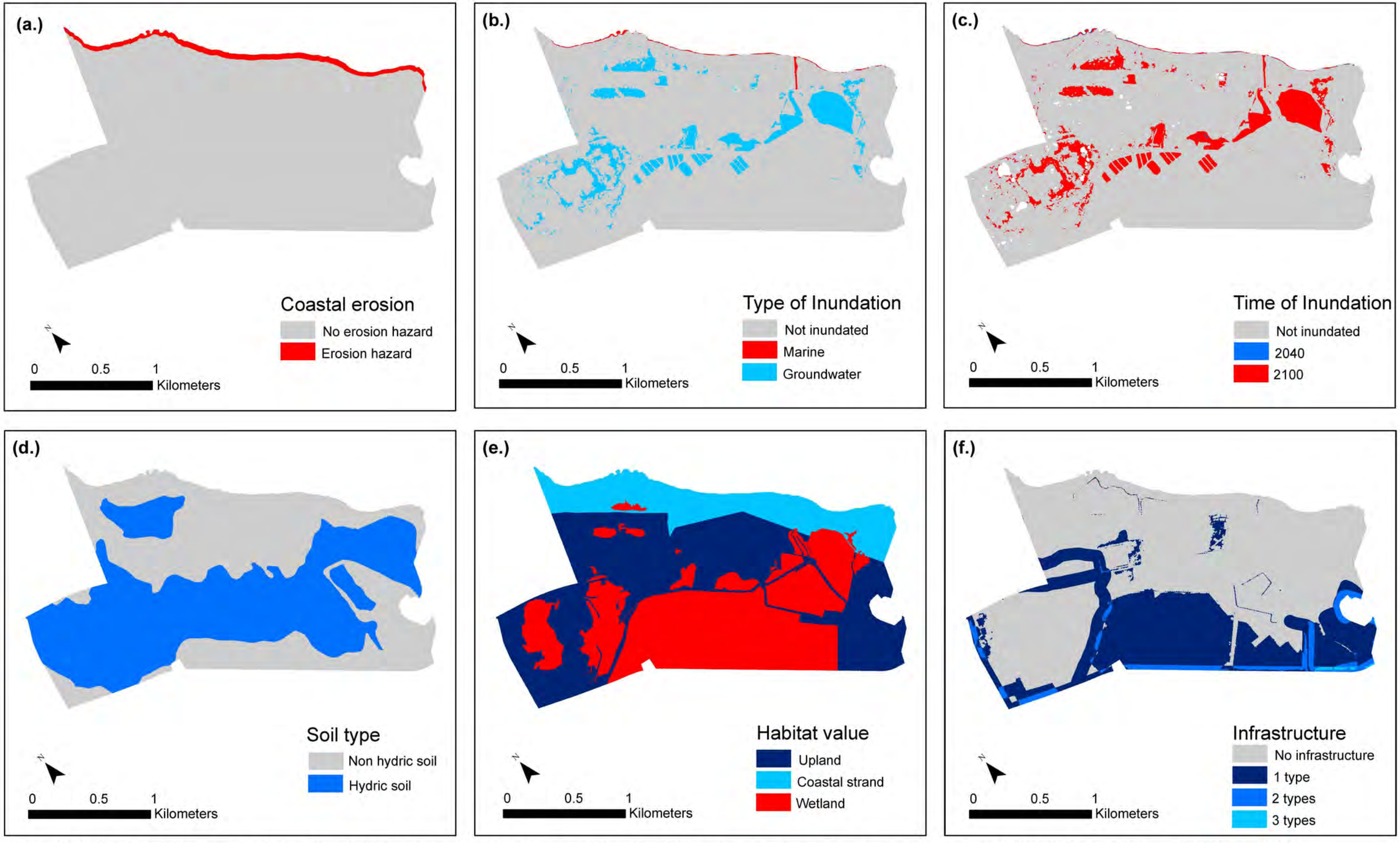

Figure 18. SLR vulnerability maps for James Campbell considering high confidence (80% probability) inundation areas under the best case scenario (B1: 0.30 m by 2040 and 1.04 m by 2100). Vulnerability at James Campbell is defined by six input parameters; coastal erosion (a), inundation type (b), time of inundation (c), soil type (d), habitat value (e), and infrastructure (f).

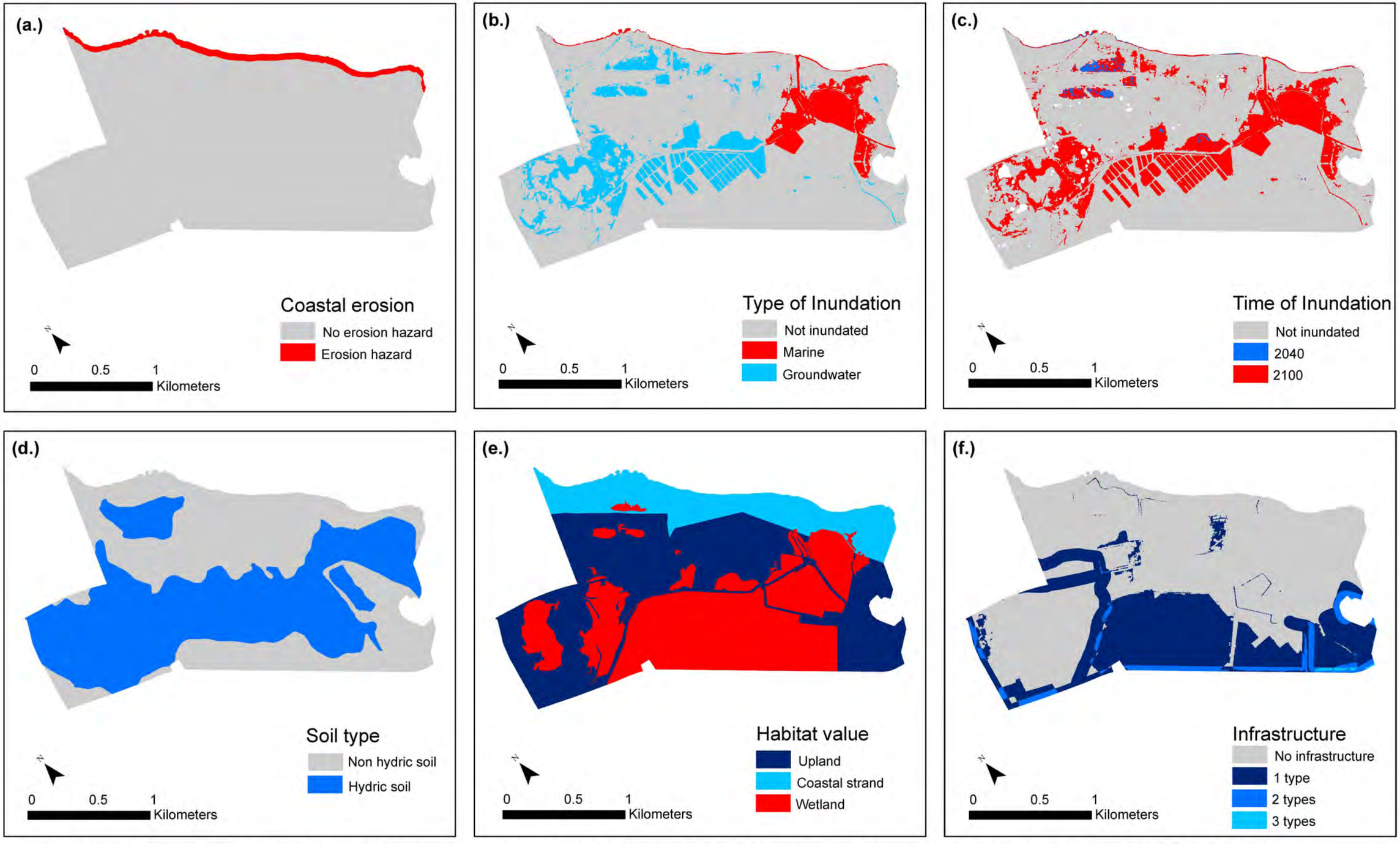

Figure 19. SLR vulnerability maps for James Campbell considering low confidence (50% probability) inundation areas under the best case scenario (B1: 0.30 m by 2040 and 1.04 m by 2100). Vulnerability at James Campbell is defined by six input parameters; coastal erosion (a), inundation type (b), time of inundation (c), soil type (d), habitat value (e), and infrastructure (f).

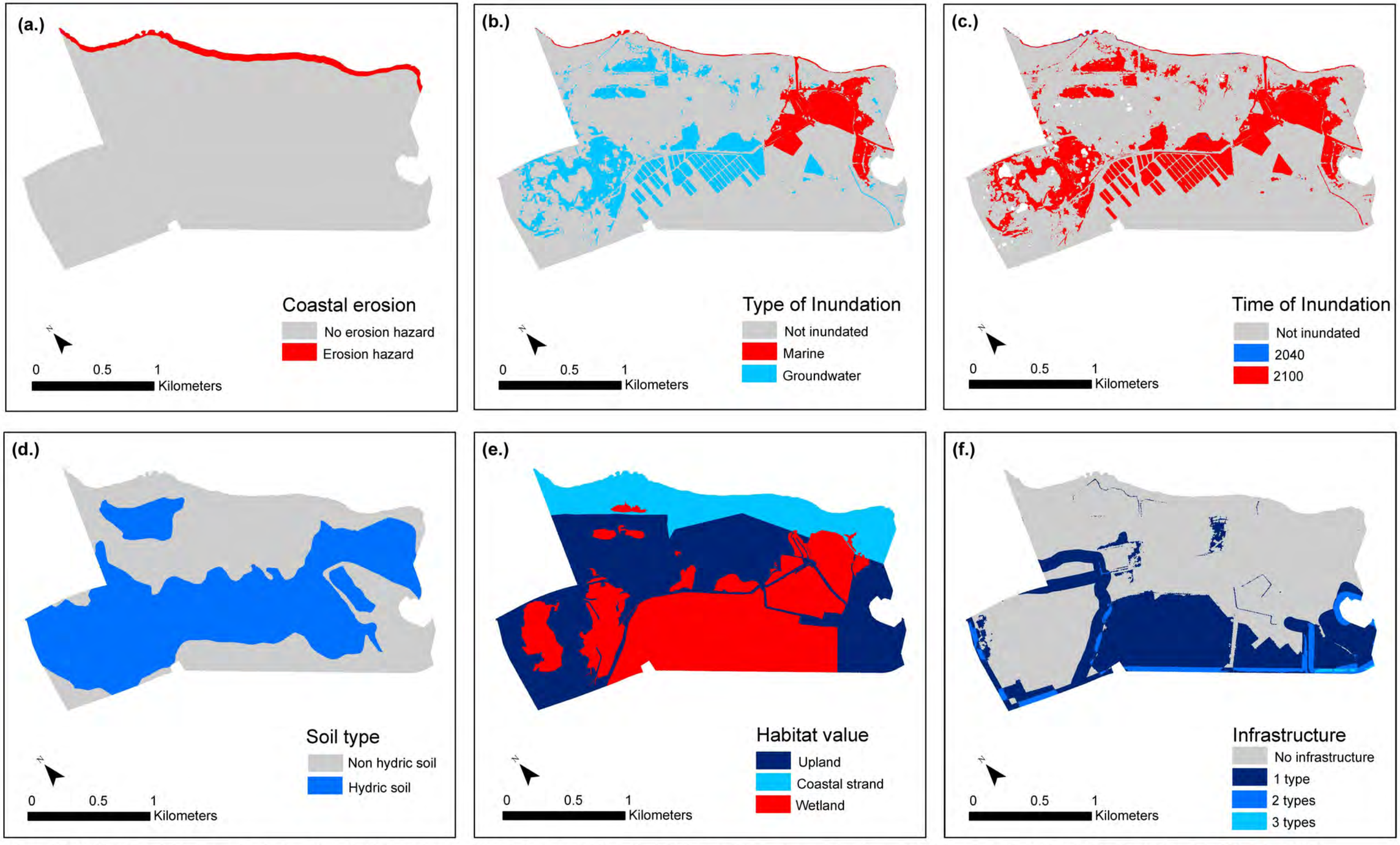

Figure 20. SLR vulnerability maps for James Campbell considering high confidence (80% probability) inundation areas under the worst case scenario (A1FI: 0.30 m by 2040 and 1.43 m by 2100). Vulnerability at James Campbell is defined by six input parameters; coastal erosion (a), inundation type (b), time of inundation (c), soil type (d), habitat value (e), and infrastructure (f).

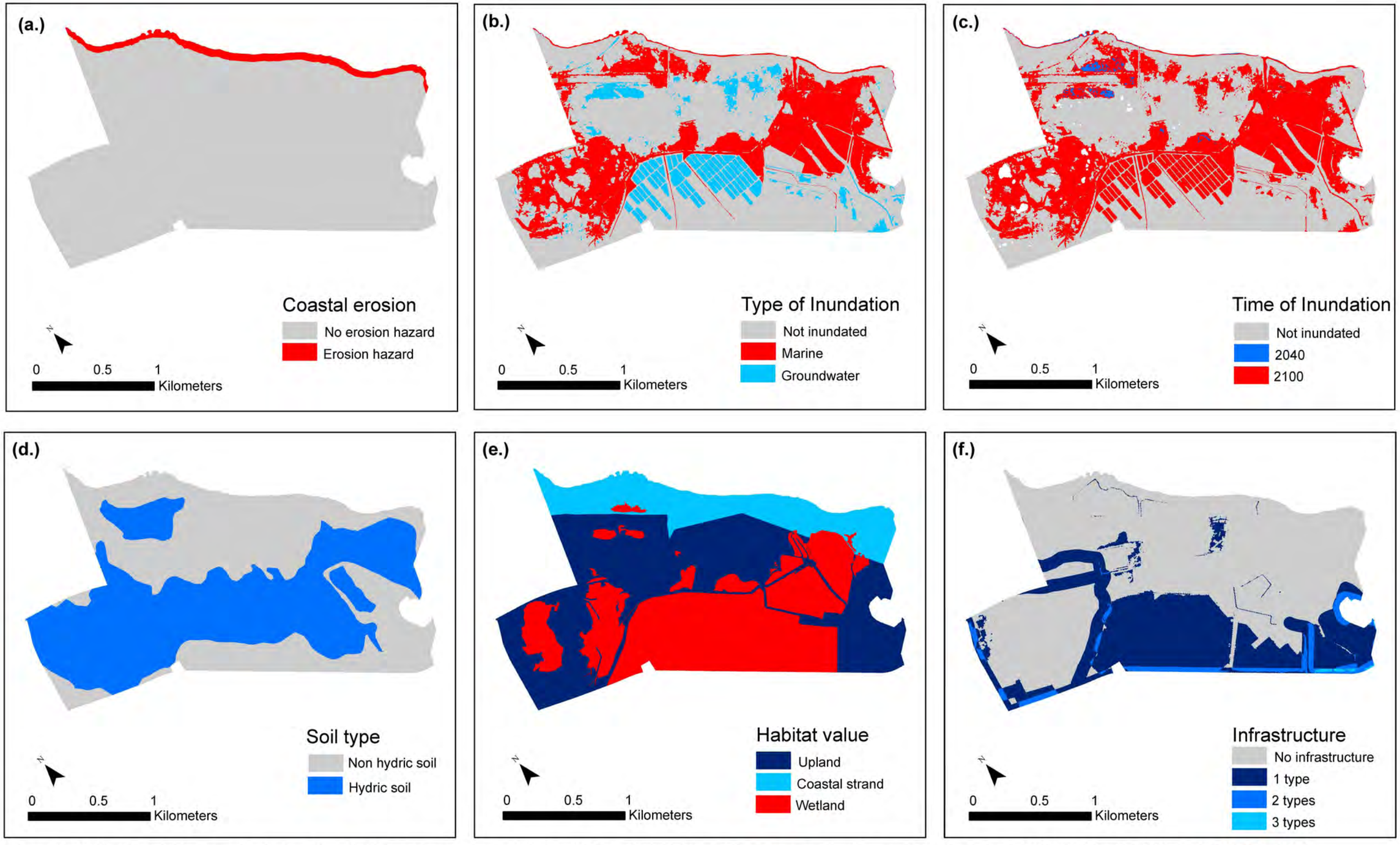

Figure 21. SLR vulnerability maps for James Campbell considering low confidence (50% probability) inundation areas under the worst case scenario (A1FI: 0.30 m by 2040 and 1.43 m by 2100 Vulnerability at James Campbell is defined by six input parameters; coastal erosion (a), inundation type (b), time of inundation (c), soil type (d), habitat value (e), and infrastructure (f).

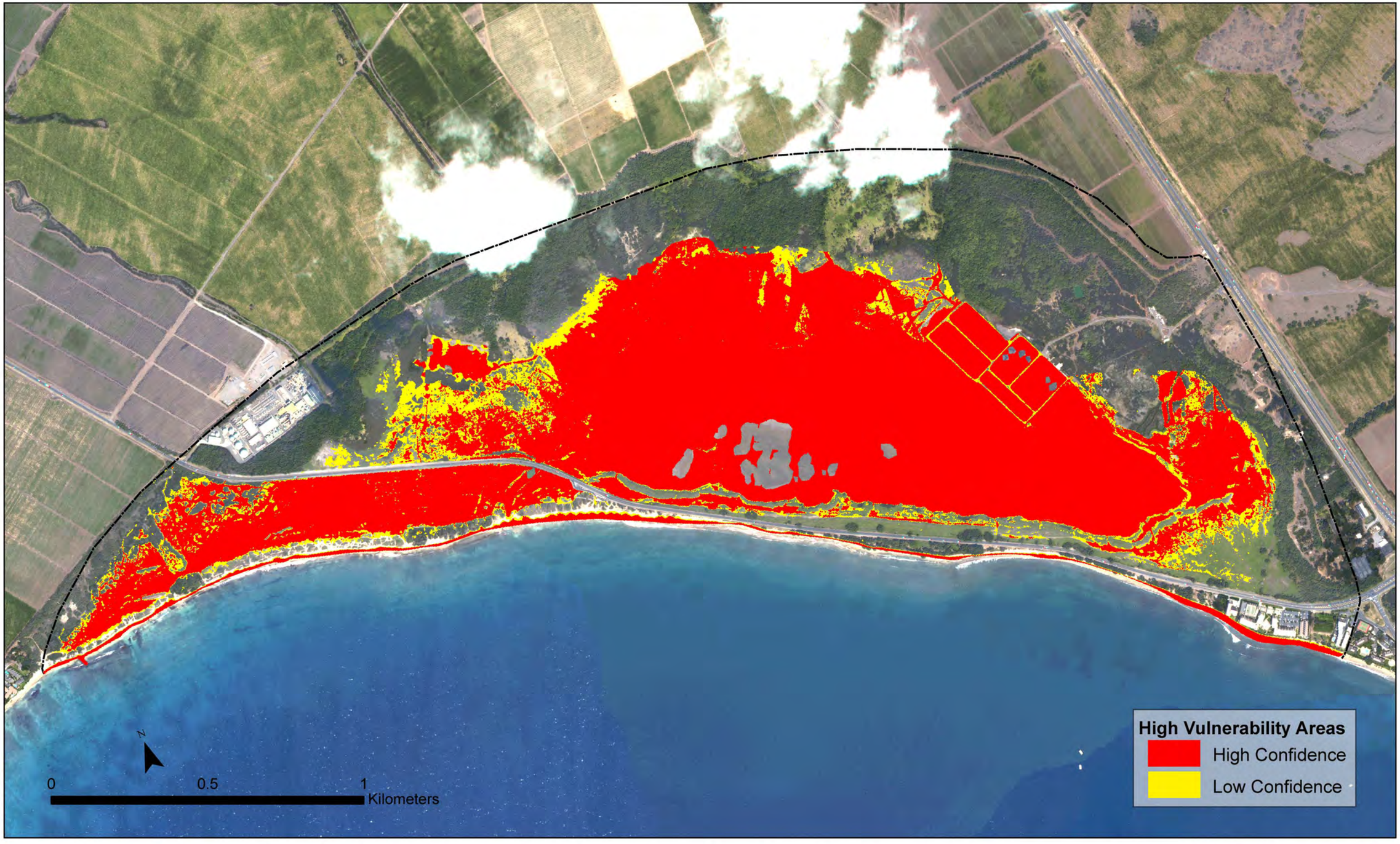

Figure 31. High vulnerability areas at Keālia mapped at high confidence (80% probability), and low confidence (50% probability) assuming a best case SLR scenario (B1: 0.30 m by 2040, 1.04 m by 2100).

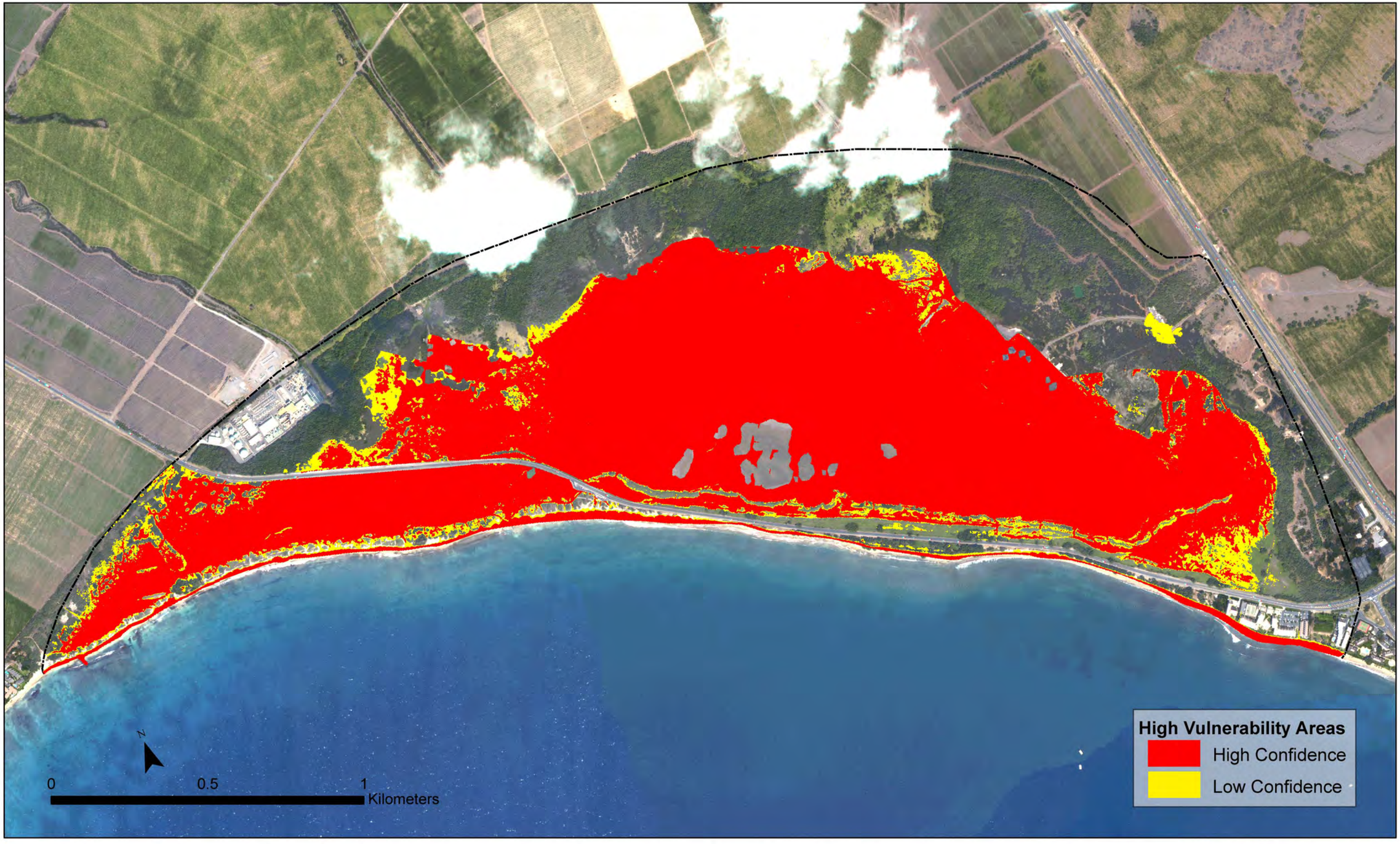

Figure 32. High vulnerability areas at Keālia mapped at high confidence (80% probability), and low confidence (50% probability) assuming a worst case SLR scenario (A1FI: 0.30 m by 2040, 1.43 m by 2100).

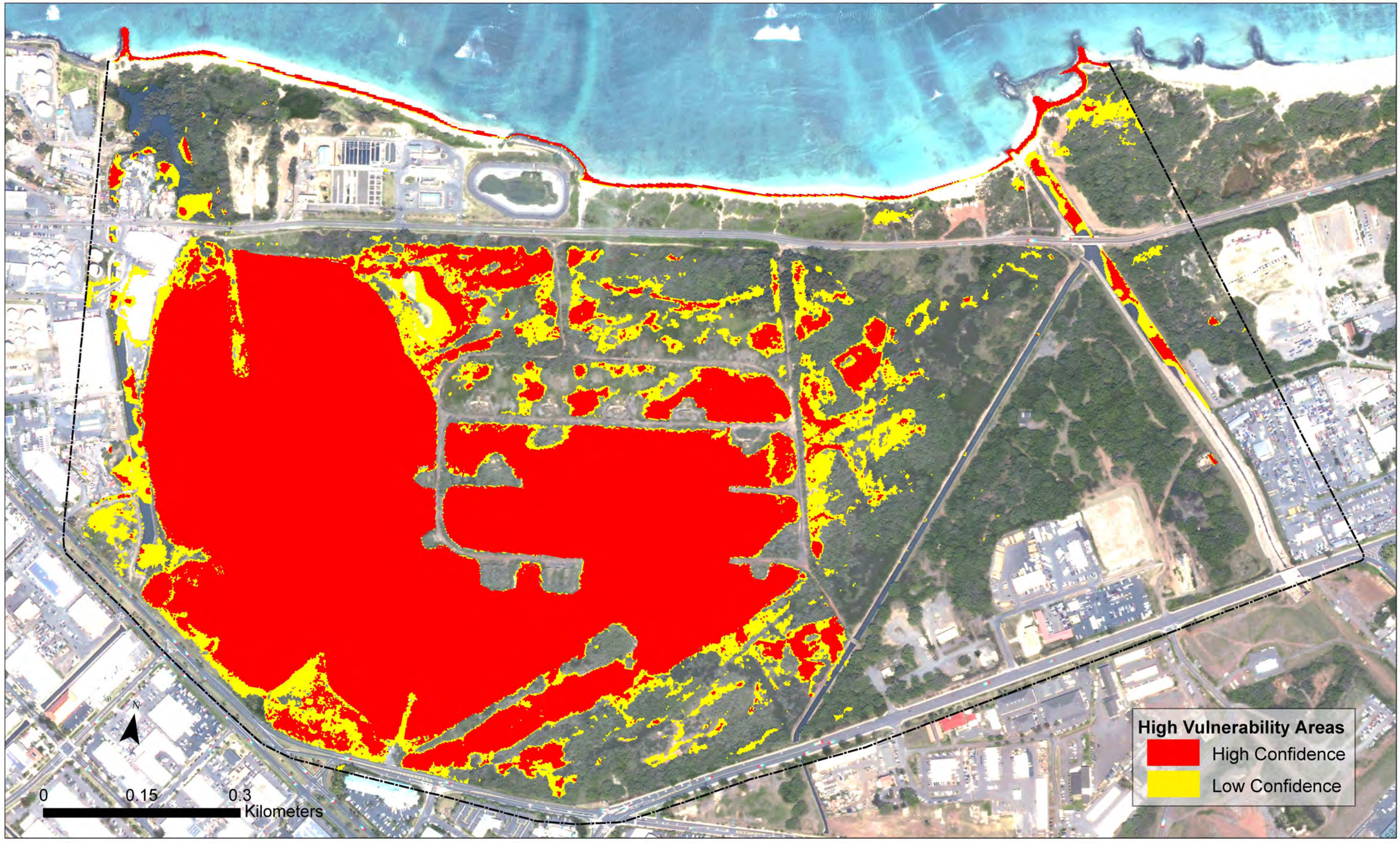

Figure 33. High vulnerability areas at Kanaha mapped at high confidence (80% probability), and low confidence (50% probability) assuming a best case SLR scenario (B1: 0.30 m by 2040, 1.04 m by 2100).

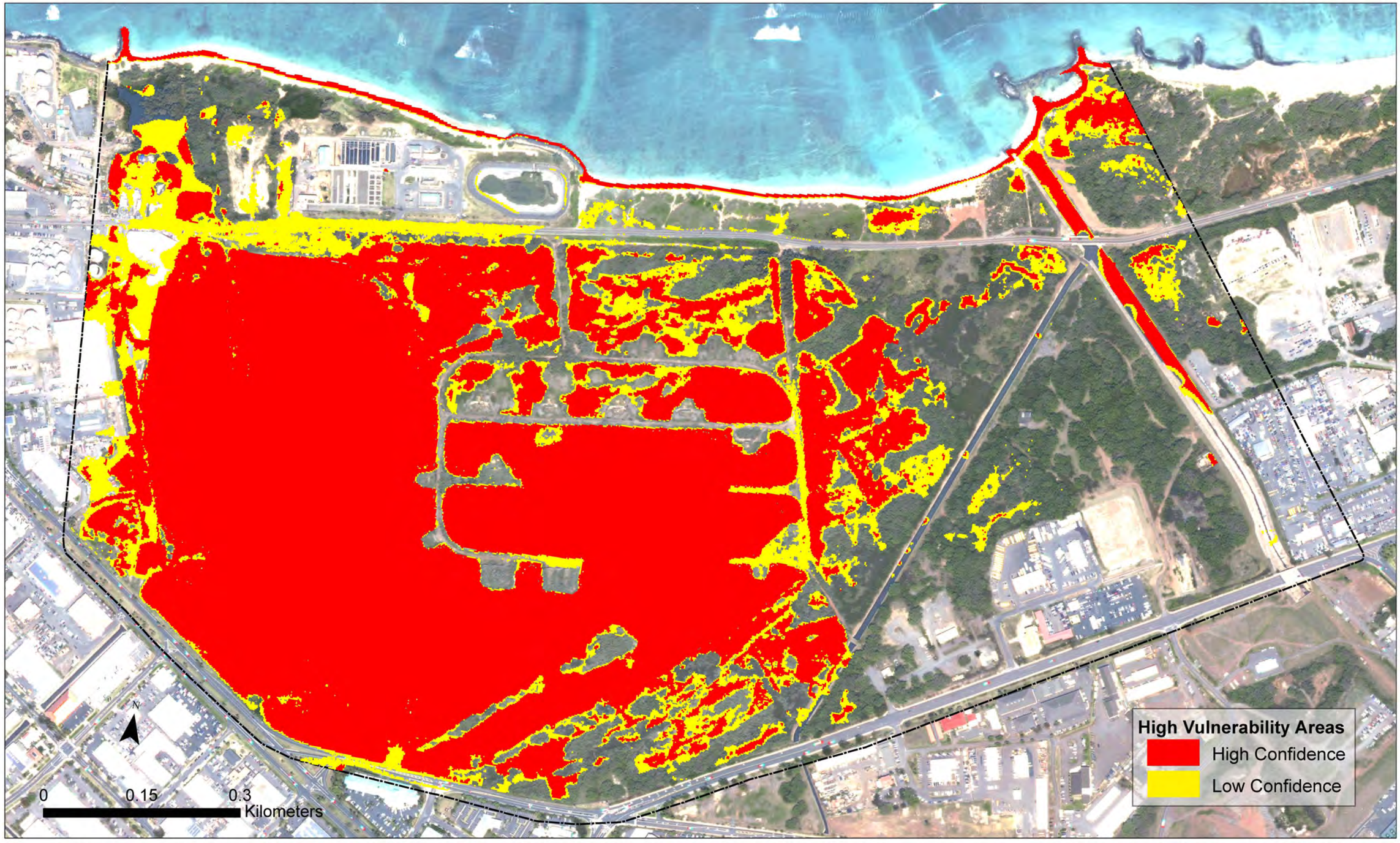

Figure 34. High vulnerability areas at Kanaha mapped at high confidence (80% probability), and low confidence (50% probability) assuming a worst case SLR scenario (A1FI: 0.30 m by 2040, 1.43 m by 2100).

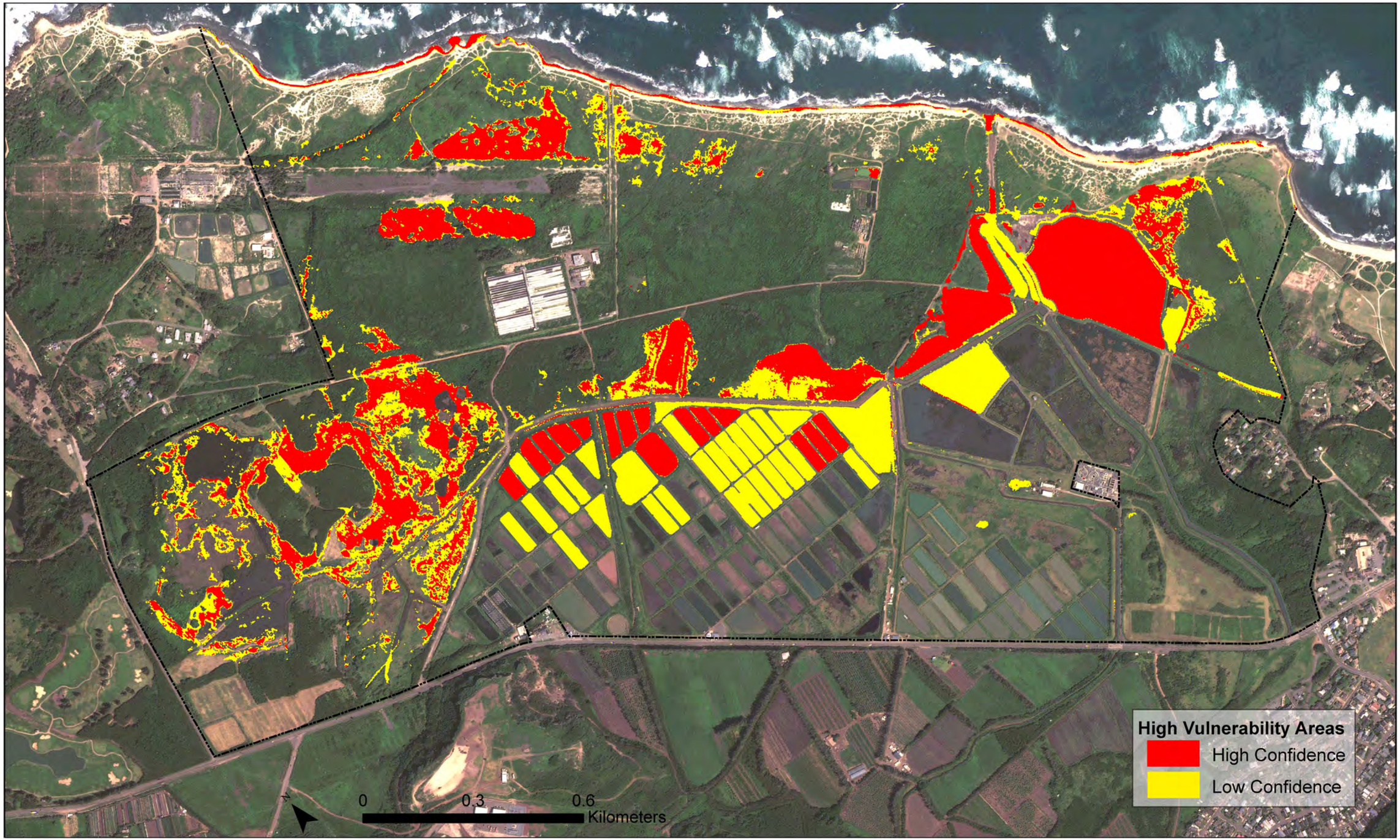

Figure 35. High vulnerability areas at James Campbell mapped at high confidence (80% probability), and low confidence (50% probability) assuming a best case SLR scenario (B1: 0.30 m by 2040, 1.04 m by 2100).

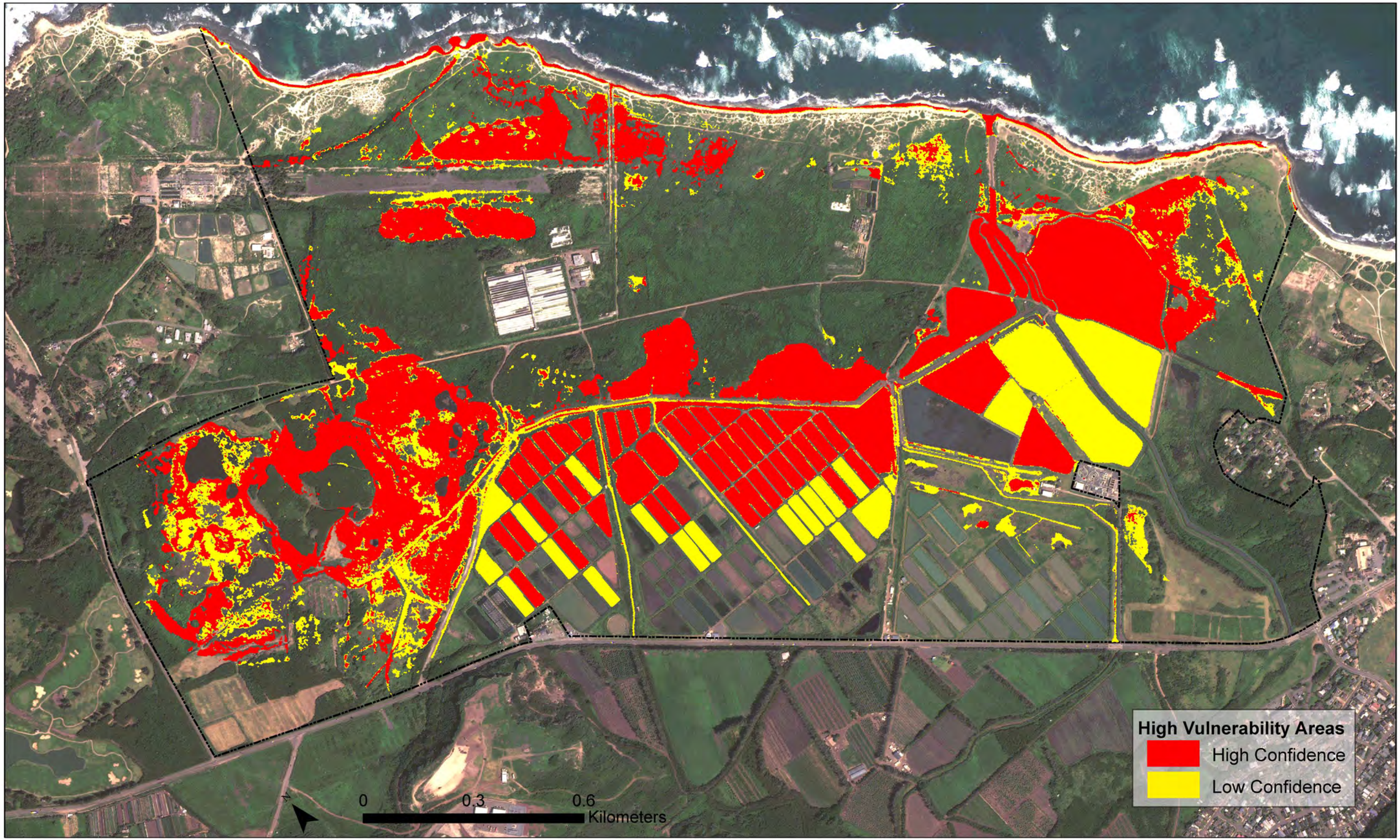

Figure 36. High vulnerability areas at James mapped at high confidence (80% probability), and low confidence (50% probability) assuming a worst case SLR scenario (A1FI: 0.30 m by 2040, 1.43 m by 2100).

B. Critical point maps

Due to the low gradient of most coastal plain environments, the rate of sea-level rise (SLR) impact will rapidly accelerate once the height of the sea surface exceeds a critical elevation. Here we develop this concept by calculating a SLR critical elevation and joint uncertainty that distinguishes between slow and rapid phases of flooding. We apply the methodology to Keālia National Wildlife Refuge (south Maui), Kanaha State Wildlife Sanctuary (north Maui), and James Campbell National Wildlife Refuge (north Oʻahu). Using high resolution LiDAR digital elevation models (DEMs) flooded areas are mapped and ranked from high (80%) to low (2.5%) risk based upon the percent probability of flooding under the B1, and A1Fl economic emissions scenarios. Figures 22-24 depict areas impacted during the slow phase, and figures 25-30 depict areas impacted during the fast phase of flooding.

Across the critical elevation, the area of wetland (expressed as a percentage of the total) at high risk of flooding under the A1Fl scenario increased from 21.0% to 53.3% (south Maui), 0.3% to 18.2% (north Maui), and 1.7% to 15.9% (north Oʻahu). At the same time, low risk areas increased from 34.1% to 80.2%, 17.7% to 46.9%, and 15.4% to 46.3%, resp. The critical elevation of SLR may have already passed (2003) on south Maui, and decision makers on North Maui and Oʻahu may have approximately 37 years (2050) to develop, and implement adaptation strategies that meet the challenges of SLR in advance of the largest impacts.

Figure 22. Area at risk under 0.2 m of SLR during the slow phase of flooding at Keālia.

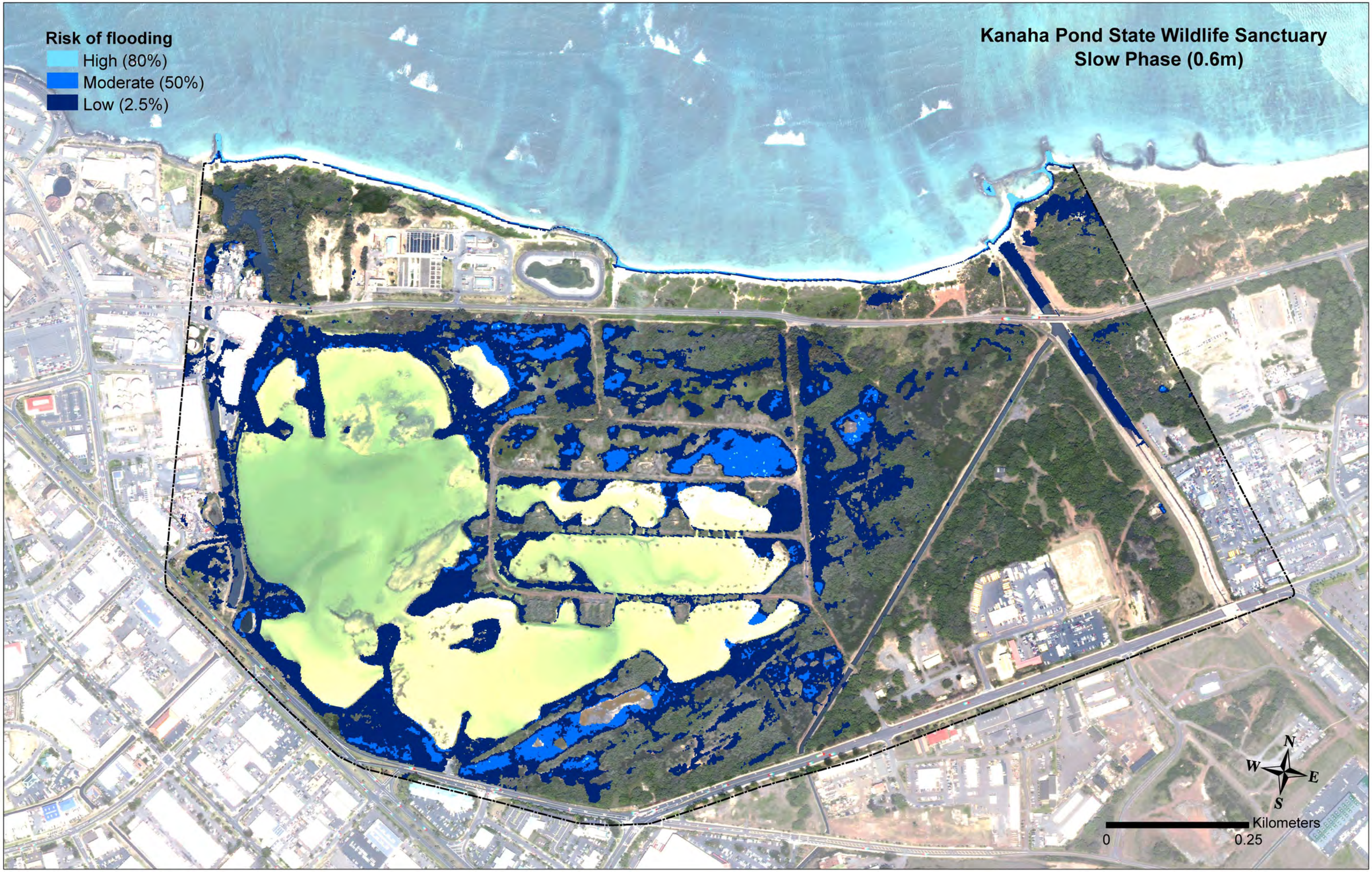

Figure 23. Area at risk under 0.6 m of SLR during the slow phase of flooding at Kanaha.

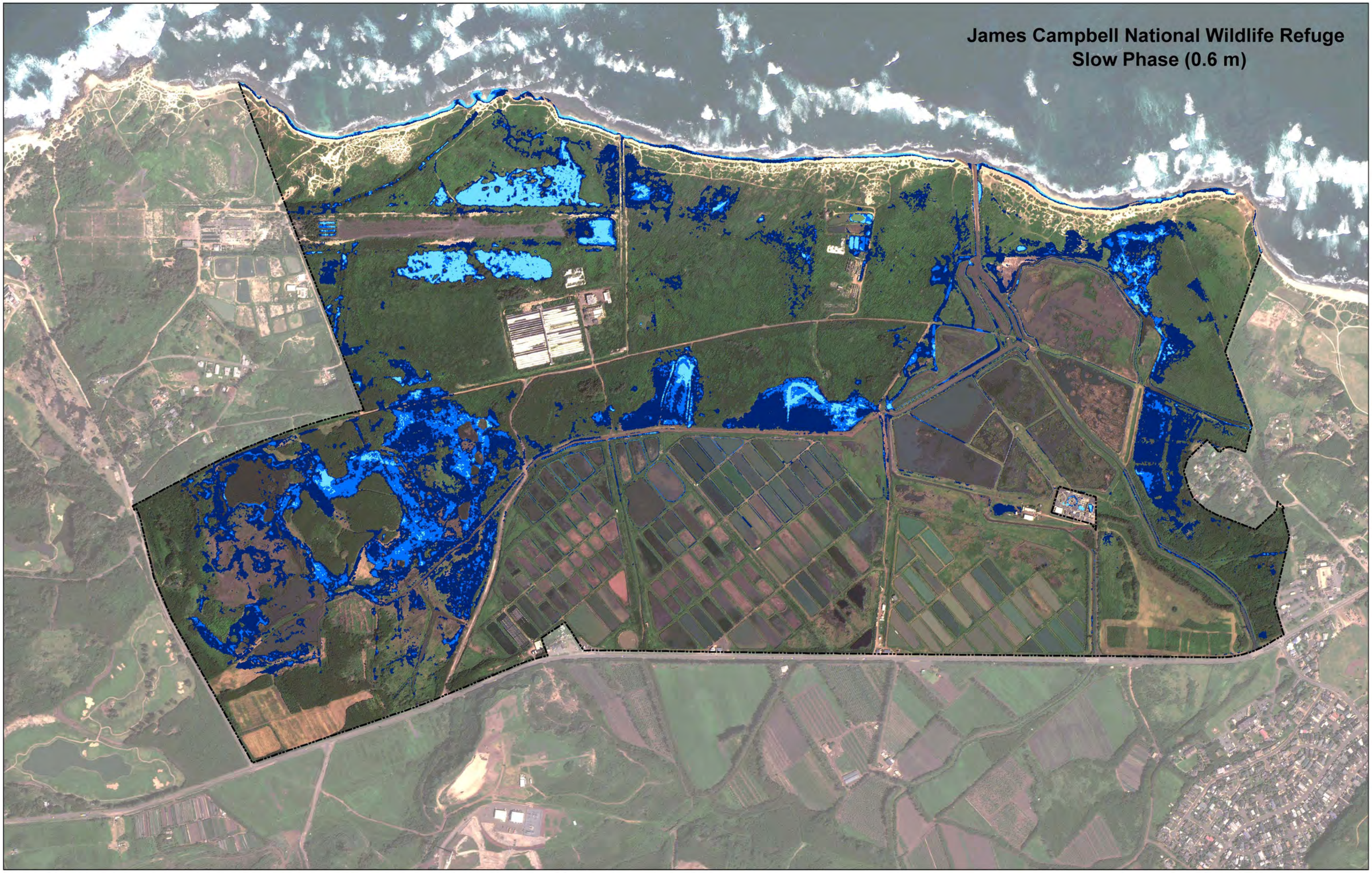

Figure 24. Area at risk under 0.6 m of SLR during the slow phase of flooding at James Campbell.

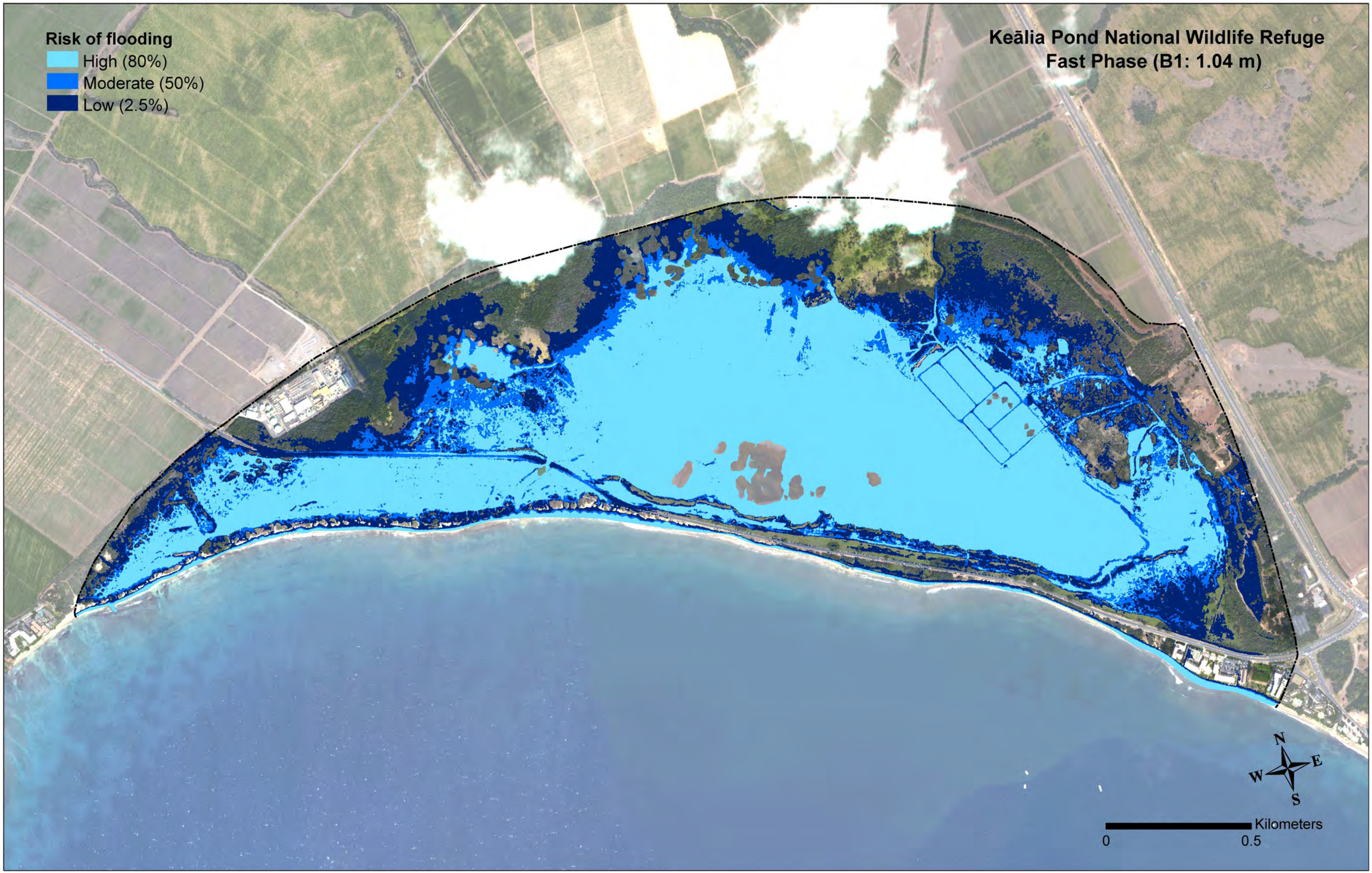

Figure 25. Area at risk under the best case (B1) 1.04 m of SLR during the fast phase of flooding at Keālia.

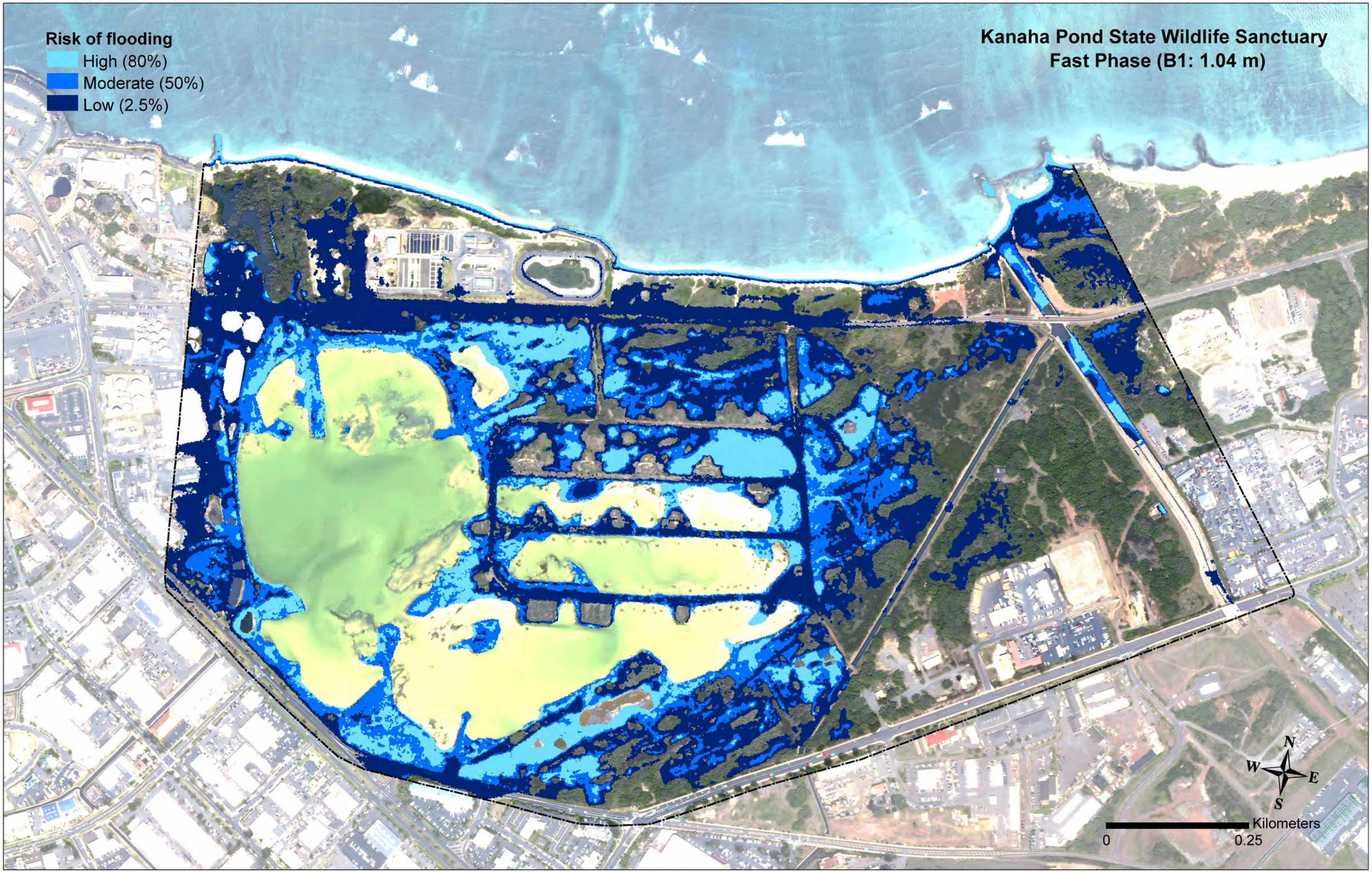

Figure 26. Area at risk under the best case (B1) 1.04 m of SLR during the fast phase of flooding at Kanaha.

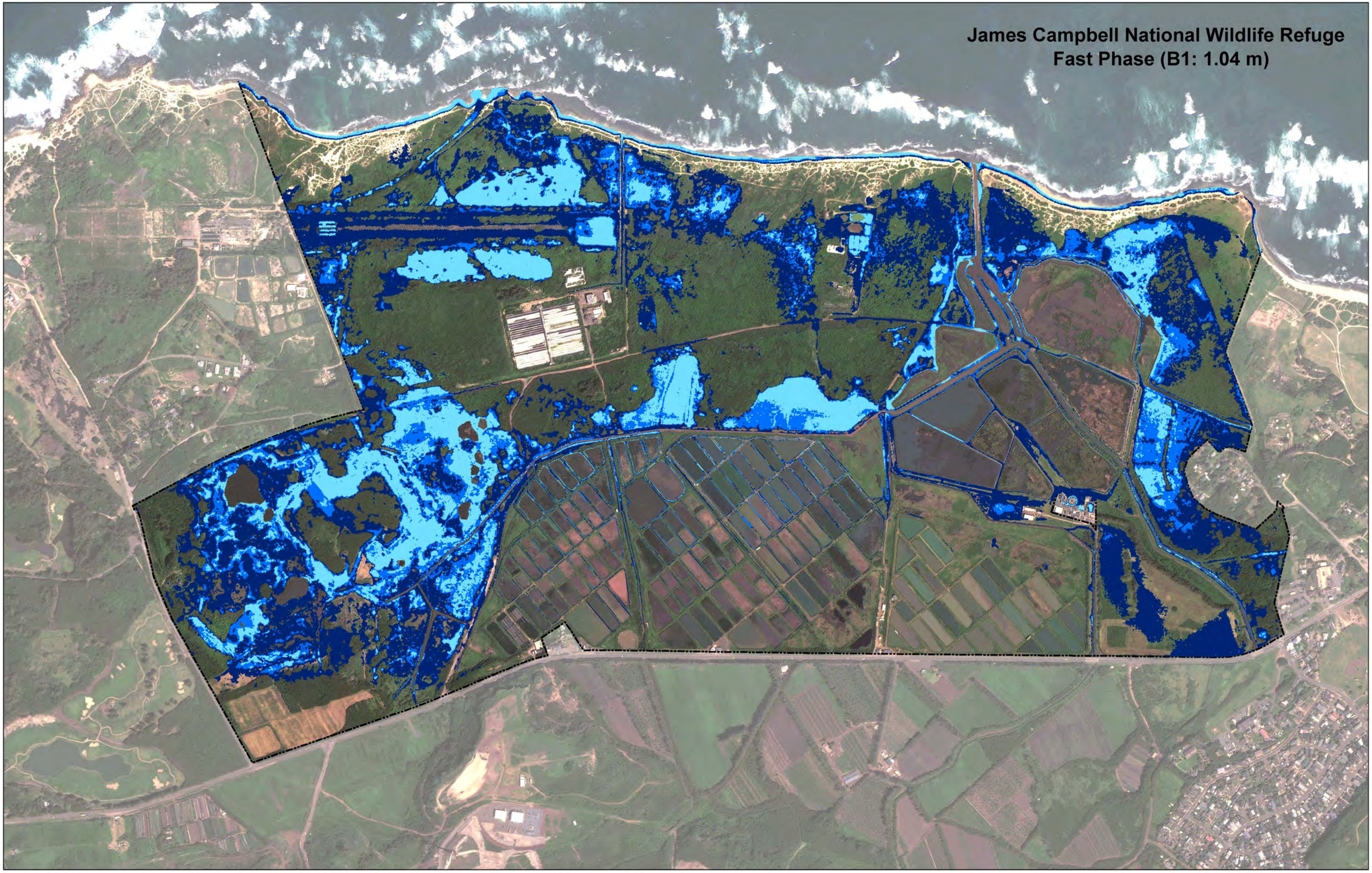

Figure 27. Area at risk under the best case (B1) 1.04 m of SLR during the fast phase of flooding at James Campbell.

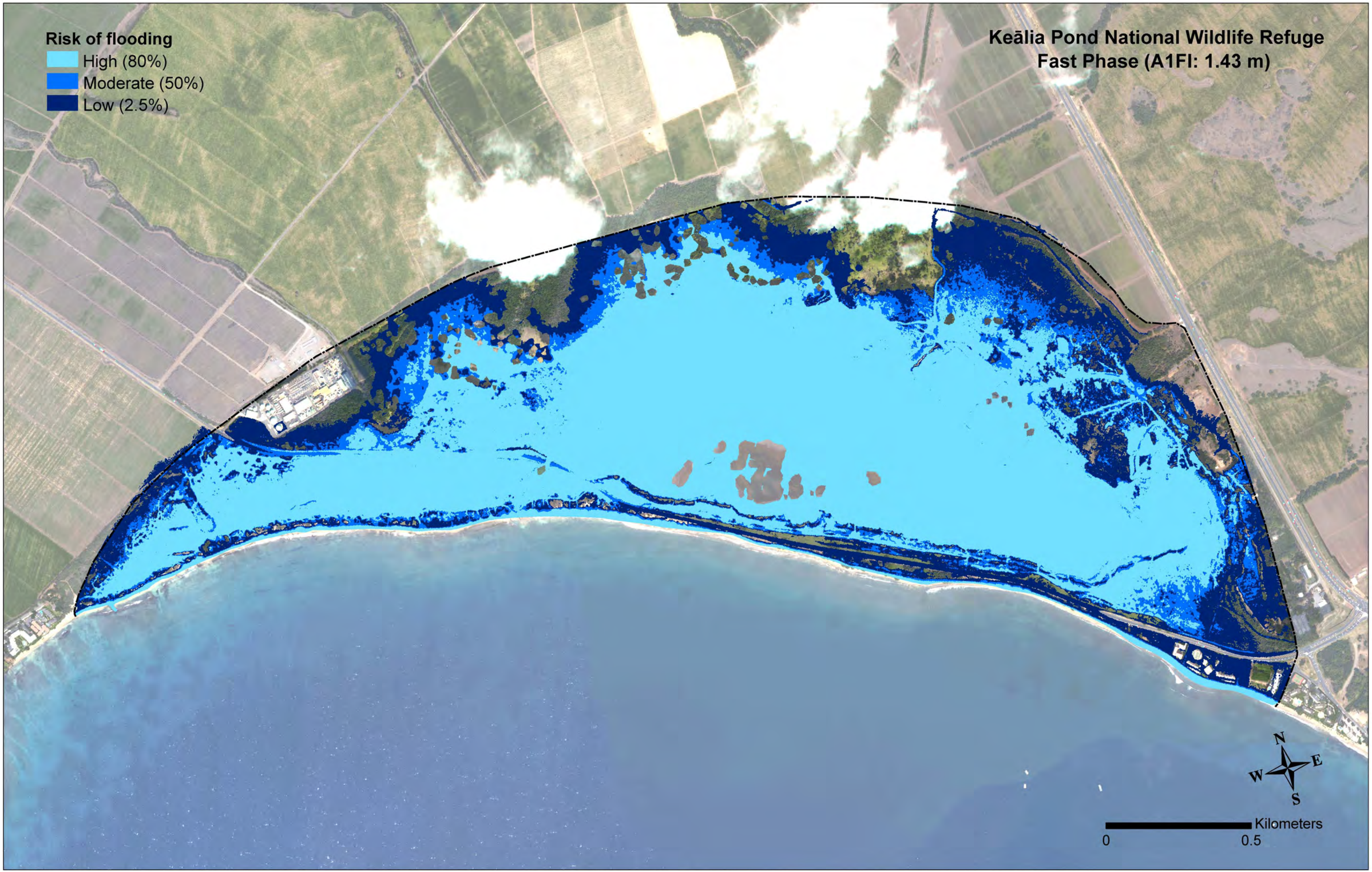

Figure 28. Area at risk under the worst case (A1FI) 1.43 m of SLR during the fast phase of flooding at Keālia.

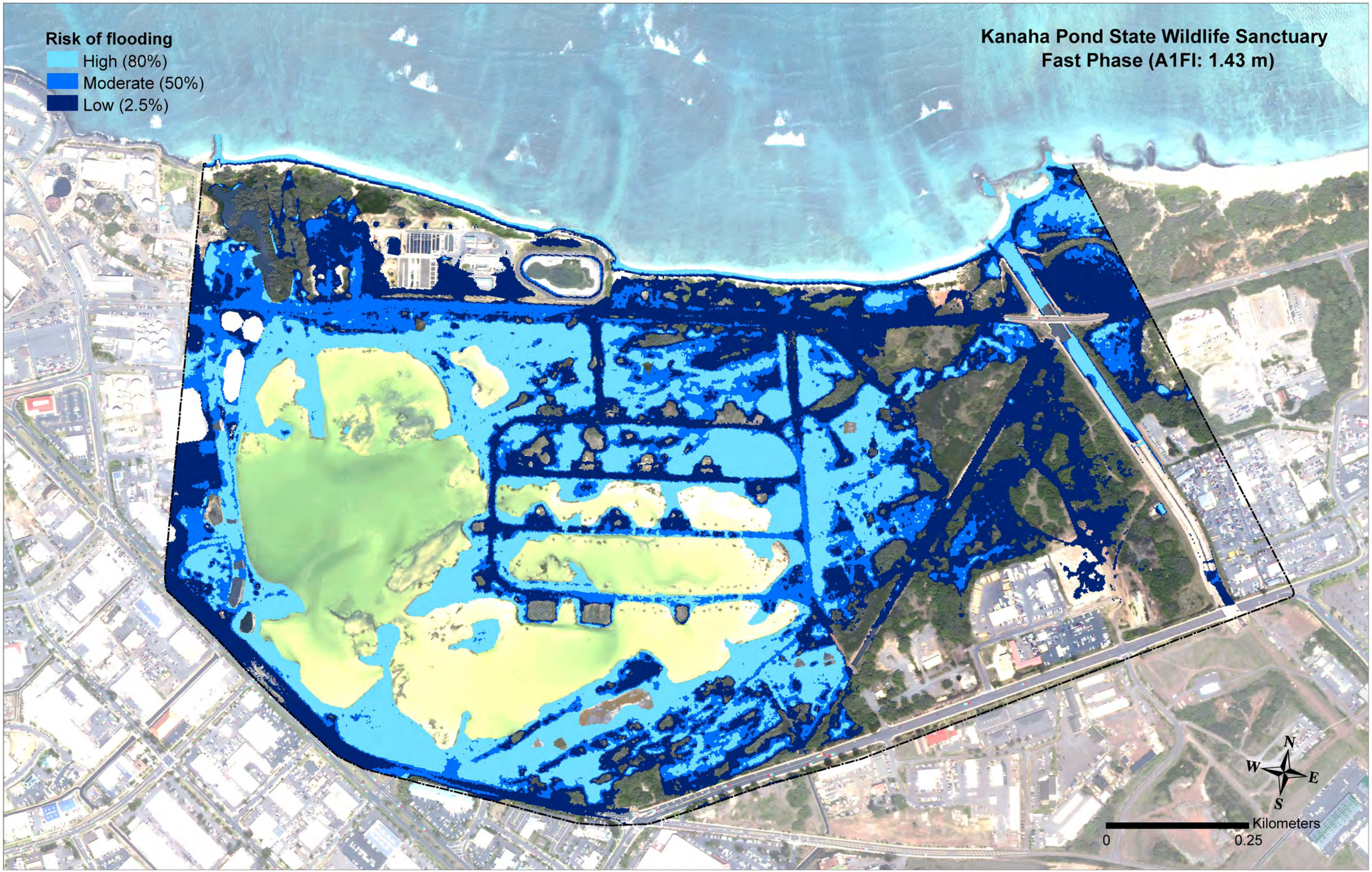

Figure 29. Area at risk under the worst case (A1FI) 1.43 m of SLR during the fast phase of flooding at Kanaha.

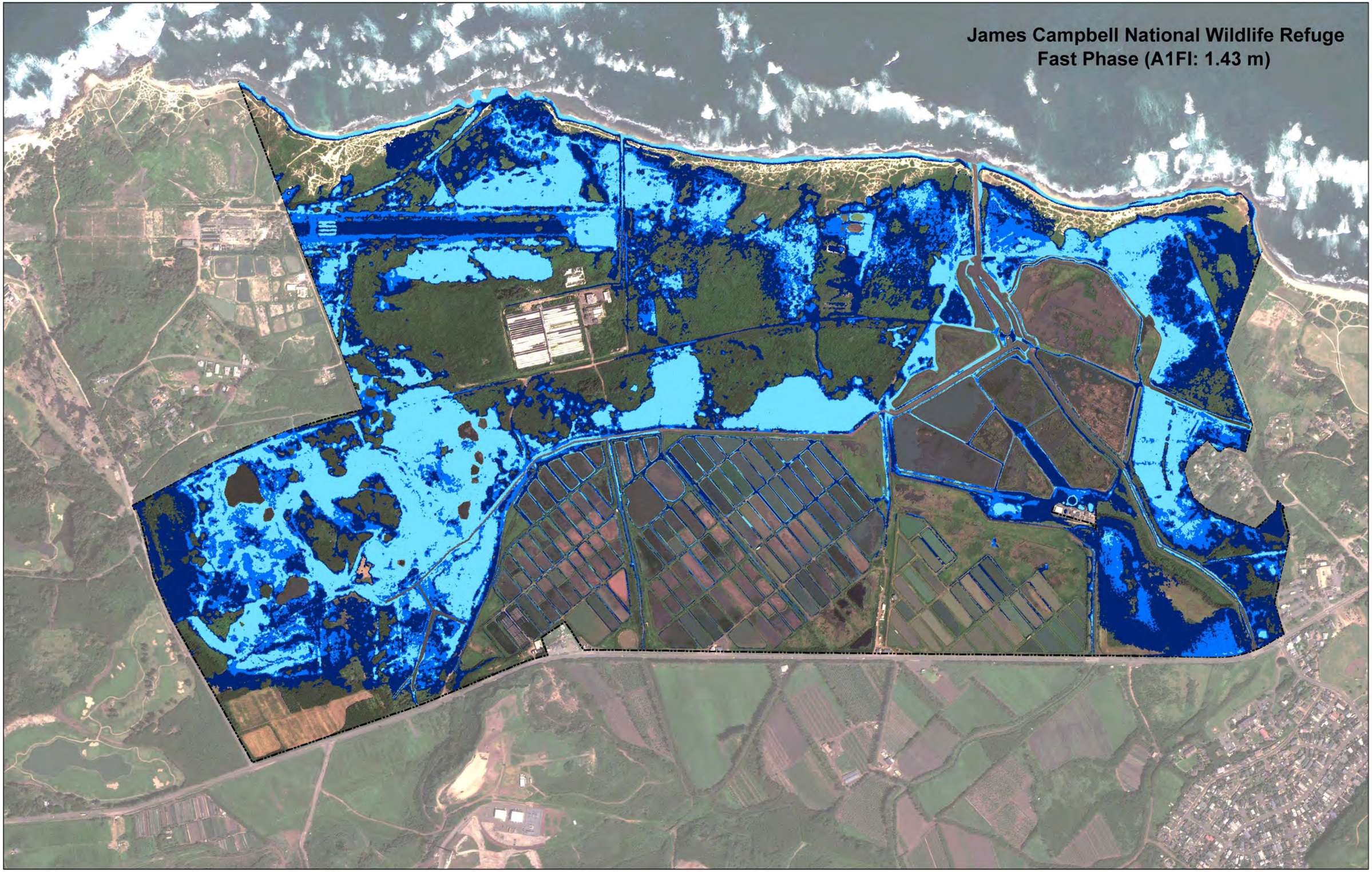

Figure 30. Area at risk under the worst case (A1FI) 1.43 m of SLR during the fast phase of flooding at James Campbell.